AIMS Mathematics, 11(4): 10274–10310.
DOI: 10.3934/math.2026425
Received: 05 March 2026
Revised: 31 March 2026
Accepted: 08 April 2026
Published: 15 April 2026

https://www.aimspress.com/journal/Math

Research article

Bilinear optimal control problem with minimum energy for a fourth-order reaction diffusion system

Mofareh Alhazmi* **and Maawiya Ould Sidi**

Department of Mathematics, College of Science, Jouf University, Sakaka, Aljouf 72341, Saudi Arabia

* **Correspondence:** Email: mmmhazmi@ju.edu.sa.

Abstract: This work was devoted to a minimum-energy optimal control problem governed by a fourth-order reaction–diffusion equation in which the control acts through a drift term. Such bilinear control problems arise naturally in transport phenomena and higher-order diffusion models, but their analysis is challenging because of the nonlinear coupling between the state and the control, as well as the difficulty of characterizing controls that are truly optimal with respect to energy. To overcome this difficulty, we formulated a family of penalized optimal control problems and characterized the minimum energy control as the limit of their solutions. The analysis was based on the associated optimality system, involving the state and adjoint equations, together with tools from convex optimization. Under appropriate assumptions, we established the existence and uniqueness of the optimal control, which provides a well-posed framework for the problem under consideration. For the numerical approximation, the resulting optimality system was solved by means of a conjugate gradient algorithm that requires, at each iteration, only the solution of the state equation and the adjoint equation. Numerical simulations showed a clear decrease in the tracking error and indicated that the computed state approaches the desired configuration with a small relative error after convergence. These results confirmed the stability, accuracy, and efficiency of the proposed approach for the minimum-energy control of fourth-order advection–reaction–diffusion systems.

Keywords: optimal control; minimum energy control; reaction–diffusion equation; bilinear control; adjoint method; convex optimization; uniqueness of optimal control; conjugate gradient method; numerical simulations
Mathematics Subject Classification: 35F50, 49M05, 49M25, 93C10

1. Introduction

Optimal control problems governed by partial differential equations (PDEs) are central to the modeling and regulation of distributed parameter systems in physics, engineering, environmental sciences, and biological processes. The mathematical foundations for optimal control of the systems described by PDEs were established in the pioneering work of Lions [1, 2].

The fundamental results on boundary problems and regularity theory were then developed by Lions and Magenes [3, 4]. Since then, the theory has undergone important developments concerning the existence of solutions, optimality conditions, and numerical methods; see, in particular, [5, 6]. The functional analysis tools needed to study PDEs were presented in the book by Brezis [7], while the issues of controllability and observability were extensively studied by Zuazua [8].

In many practical applications, additive controls act as external source terms and, therefore, do not change the intrinsic properties of the system. This limitation has led to the development of bilinear or multiplicative control problems in which control appears as a coefficient of the governing equation. Such formulations make it possible to act directly on essential physical mechanisms, such as transport, diffusion, or reaction rates. Khapalov [9] proposed a systematic study of the multiplicative controllability of PDEs. The controllability properties of the bilinear reaction scattering equations were analyzed by Cannarsa et al. [10]. The bilinear optimal control applied to quantum systems was studied by Ito and Kunisch [11]. The regional controllability of distributed bilinear systems was introduced by Zerrik and Ould Sidi [12], and then extended to the problems of optimal regional control by Ztot et al. [13].

Drift field control models appear naturally in environmental applications related to the transport of pollutants. In these systems, the evolution of the pollutant concentration is governed by the combined phenomena of diffusion and advection, while the control action may correspond to the modification of an imposed velocity field, generated, for example, by pumping or artificial circulation devices. The control of the drift field thus makes it possible to redistribute pollutants within the domain without introducing new sources. Such modeling approaches have been used, in particular, in groundwater remediation problems [14]. The controllability and numerical processing of transport processes described by advection-diffusion equations were then studied in the framework of distributed parameter systems [15]. Stabilized optimal control methods for convection-diffusion equations, frequently encountered in environmental transport models, were analyzed in [16].

From a numerical point of view, several works have focused on the bilinear optimal control governed by convection-diffusion equations. Stabilized finite element methods were studied by Becker and Vexler [17]. A priori error estimates for bilinear state equations were established by Kröner and Vexler [18]. Efficient multigrid optimization methods were proposed by Borzí et al. [19]. The optimal control of the Fokker–Planck equations was studied by Fleig and Guglielmi [20]. More recently, Glowinski et al. [21] presented the variational methods for the numerical solution of nonlinear elliptic problems.

Recent developments have extended the theory of optimal bilinear control to more complex models. The bilinear control involving fractional operators was studied by Bersetche et al. [22]. The degenerate parabolic equations were analyzed by Kenne [23]. Problems with incomplete data were considered by Ahab et al. [24], while systems with unbounded control operators were studied by El Boukhari and Zerrik [25]. Very recent contributions also refer to the fractional scattering models studied by

Mophou et al. [26, 27] and the problems of punctual pursuit analyzed by Otárola et al. [28]. Recent developments on inverse problems associated with fractional diffusion and diffusion–wave equations governed by nonlocal operators have also attracted significant attention; see, for instance, [29]. Recent developments in the study of optimal control problems for reaction–diffusion–convection equations can be found in the work of Baranovskii, Brizitskii, and Saritskaia [30], where solvability results were established for weak and strong solutions in a variable-coefficient framework. Optimal control theory has also addressed various classes of fractional and functional differential systems. [31] dealt with optimal control results for fractional differential hemivariational inequalities of order $r \in (1, 2)$. [32] was devoted to optimal control strategies and continuous dependence for stochastic Hilfer fractional systems with delay in a Volterra–Fredholm integro-differential setting. In [33], the authors studied optimal control and approximate controllability for fractional integrodifferential evolution equations with infinite delay. These works further highlight the current activity in optimal control for nonclassical systems and enrich the general background of the present study.

Conjugate gradient methods play an important role in optimal control problems, especially for large-scale systems governed by partial differential equations. Their efficiency is mainly due to their computational efficiency, their ability to exploit gradient information without the need for explicit computation of second-order derivatives, and their improved convergence behavior compared to standard gradient descent methods. In PDE-constrained optimization, where the gradient of the cost functional is typically obtained through state and adjoint systems, the conjugate gradient framework provides a natural and efficient numerical strategy [15]. In contrast, in recent years, interest in fractional gradient-based optimization methods has emerged for various applications, including nonlinear system estimation, adaptive processing, and signal analysis. These developments show that fractional gradient techniques are an important emerging trend in optimization and computational methods. In this context, it is useful to mention these approaches in order to offer the reader a broader perspective on recent developments related to gradient-based numerical procedures [34, 35].

Research Gap: Despite these advances, minimum-energy optimal control problems governed by fourth-order advection–reaction-diffusion equations with bilinear drift control remain largely unexplored. Most of the existing work is based on tracking-type cost functionals and often relies on the assumption of incompressibility $\nabla \cdot \mathbf{m} = 0$. In contrast, the characterization of a minimum-energy control through the limit of a family of penalized problems, as well as the analysis of the uniqueness of the corresponding optimal solution, remains open for this class of models.

Contributions: The objective of this work is to investigate an optimal control strategy for a fourth-order advection–reaction–diffusion system in which the control acts through a drift mechanism. The proposed approach combines theoretical analysis and numerical investigation in order to better understand both the qualitative properties of the optimal control and its practical computational behavior. In particular, special attention is paid to the stabilization of the control after convergence and to the reduction of control energy observed in the numerical simulations. The main contributions of the present study are summarized as follows.

Theoretical contributions

1. We formulate an optimal control problem associated with a fourth-order advection–reaction–diffusion model involving a drift-type control acting in the transport term.

2. The well-posedness of the state equation is established under suitable assumptions on the system parameters and admissible controls.
3. A minimum-energy optimal control framework is introduced that ensures both trajectory tracking and control regularization.
4. The first-order optimality system is derived by means of the associated adjoint equation.
5. Under a suitable additional condition, we prove the uniqueness of the optimal control. This result is important both analytically and numerically, since it reinforces the well-posedness of the problem and supports the convergence of the proposed algorithm.

Numerical contributions

1. A numerical procedure is developed to detect the convergence of the controlled system using a tracking-error criterion.
2. A post-convergence control regime is proposed, showing that the control magnitude can be reduced once the desired trajectory has been achieved.
3. The temporal evolution of the control norms is analyzed, providing numerical evidence of stabilization and reduction of control energy.
4. Spatial comparisons before and after convergence highlight the transition toward smoother and weaker control distributions.
5. The numerical results illustrate not only the implementation of the method, but also its theoretical relevance. Indeed, the decay of the absolute and relative tracking errors confirms the convergence and stability of the proposed algorithm, while the energy comparison between m_ϵ and its limit control m_0 over the interval $(0, 1)$ shows that the limiting procedure effectively selects a lower-energy control. This numerical evidence is fully consistent with the minimum-energy perspective developed in the paper.

The remainder of this article is organized as follows. In Section 2, we present the mathematical formulation of the optimal control problem associated with the fourth-order advection–reaction-diffusion system. Section 3 is devoted to the study of the existence of solutions for the penalized problem. In Section 4, we establish the characterization of the optimal control using the optimality system obtained by the adjoint method. Section 5 analyzes the passage to the limit when the parameter of criminalization tends to zero, making it possible to obtain the problem of control at the minimum energy. Section 6 describes the proposed numerical approach based on a conjugate gradient method to resolve the control problem. Finally, Section 7 presents numerical experiments that illustrate the stability, convergence, and efficiency of the proposed method.

2. Formulation of the problem

Let $\Theta \subset \mathbb{R}^q$ $(q \geq 1)$ be a bounded domain with boundary $\partial\Theta$ of class C^2. For $T > 0$, we denote by $D = \Theta \times (0, T)$, $\vartheta = \partial\Theta \times [0, T]$. The spatiotemporal admissible control set is defined by

$$\mathcal{M} = \left\{ \boldsymbol{m} \mid \boldsymbol{m} \in L^2(D), \nabla m \in L^\infty(D) \text{ and } \iint_D |\varphi - \varphi_d|^2 \, dxdt \text{ is small} \right\},$$

where the target function φ_d is given in $L^2(D)$ and $\varphi = \varphi(t; \boldsymbol{m})$ is the output of the considered advection–reaction–diffusion system defined by

$$\begin{cases} \dfrac{\partial \varphi}{\partial t} - \alpha \Delta^2 \varphi + m \cdot \nabla \varphi + a\varphi = g \quad \text{in } D = \Theta \times (0, T), \\ \varphi(x, 0) = \varphi_0 \quad \text{in } \Theta, \\ \varphi(x, t) = \dfrac{\partial \varphi(x, t)}{\partial \nu} = 0 \quad \text{in } \vartheta = \partial\Theta \times (0, T), \end{cases} \tag{2.1}$$

where the bi-Laplacian

$$\Delta^2 : H_0^2(\Omega) \to H^{-2}(\Omega)$$

is a bounded linear operator between the Sobolev spaces $H_0^2(\Omega)$ and $H^{-2}(\Omega)$, and ∇ represents the spatial gradient operator; see [3]. The diffusion coefficient $\alpha > 0$ and the reaction parameter a are taken to be constants. Moreover, the data satisfy $g \in L^2(D)$, $\varphi_0 \in L^2(0, T; H^{1/2}(\partial\Theta))$.

Remark 2.1.

- *The constant $\alpha > 0$ denotes the biharmonic diffusion coefficient.*
- *The vector field* **m** *represents the velocity of advection (drift).*
- *The coefficient a is the reaction parameter.*
- *The function g is a distributed source term defined in $D = \Theta \times (0, T)$.*
- *The boundary conditions*

  $$\varphi = \frac{\partial \varphi}{\partial \nu} = 0 \quad \text{on } \partial\Theta \times (0, T)$$

  correspond to clamped boundary conditions, which are typical for plate-type models involving the biharmonic operator [4].

The analysis in this work is carried out for the dimensionless form of the model, and the coefficients appearing in the equation are understood as nondimensional parameters. From a physical point of view, the boundary conditions in (2.1) mean that the state is fixed on the boundary:

$$\varphi = 0 \quad \text{on } \partial\Theta \times (0, T),$$

while its normal derivative also vanishes there:

$$\frac{\partial \varphi}{\partial \nu} = 0 \quad \text{on } \partial\Theta \times (0, T).$$

Hence, the boundary is fully constrained in the sense that both the value of the state and its normal variation are prescribed to be zero. Such boundary conditions are standard for fourth-order diffusion-type models and are consistent with the higher-order structure of the system.

We emphasize that, unlike some related works [15], in the present paper, no incompressibility condition is imposed on the drift field **m**. In particular, we do not assume the divergence-free constraint

$$\nabla \cdot \mathbf{m} = 0.$$

This condition is standard in incompressible flow models and plays an important role in the analysis since it implies, after integration by parts, that

$$\int_\Theta (\mathbf{m} \cdot \nabla \varphi)\, \varphi \, dx = 0,$$

so that the convection term does not contribute to the energy balance. In that setting, the drift acts only as a transport mechanism and preserves the energy of the system.

In contrast, in the present work, we only assume that

$$\mathbf{m} \in L^{\infty}(0,T;L^2(\Theta)^q),$$

without any divergence-free restriction. This allows us to treat a broader class of controls, including genuinely space-time dependent compressible drift fields. In this case, the convection term no longer vanishes in the energy estimate. Nevertheless, it remains a lower-order term and can be handled by means of Hölder's inequality, interpolation inequalities, and Young's inequality. Because of the coercivity of the biharmonic operator, this contribution can be controlled in the energy analysis.

From the modeling point of view, the divergence-free assumption corresponds to incompressible transport, whereas the present framework accommodates more general advective mechanisms, including compressible flows and externally imposed drift fields. Therefore, our analysis applies to a wider class of bilinear controls than those covered under the incompressibility constraint.
The main goals of this work are to investigate a minimum-energy control problem (MEP)

$$\begin{cases} \boldsymbol{Min} \displaystyle\iint_Q |\boldsymbol{m}|^2 dxdt, \\ \text{Subject to } \forall \boldsymbol{m} \in \mathcal{M}. \end{cases} \tag{2.2}$$

In the energy problem (2.2), the control variable $\boldsymbol{m}$ acts as a flow velocity field in the advection term of Eq (2.1). By suitably modifying the velocity field $\boldsymbol{m}$, one can steer the system so that the state φ and its terminal state $\varphi(T)$ approximate the prescribed profiles φ_d. The optimization framework presented by (2.2) is different from that of Glowinski et al. [15], where the cost functional combines a tracking term with a penalization of the control, leading to a compromise between the approximation of the desired state and the magnitude of the control. By contrast, in the present work, we consider a family of minimization problems whose asymptotic limit allows us to characterize a control that reaches the target with minimum energy. Hence, our approach is not limited to reducing the tracking error; it also provides a variational selection of an energetically optimal control.

We define

$$V = H_0^2(\Theta) = \{\psi \in H^2(\Theta)\,;\ \psi = 0 \text{ and } \partial_\nu \psi = 0 \text{ on } \partial\Theta\}, \qquad \|\psi\|_V = \|\Delta\psi\|_{L^2(\Theta)}.$$

Let V' be the dual space of V, and we introduce

$$W(0,T) = \left\{\varphi \in L^2(0,T;V)\,;\ \partial_t\varphi \in L^2(0,T;V')\right\}.$$

The variational formulation of (2.1) reads as follows: Find $\varphi \in W(0,T)$ such that $\varphi(0) = \varphi_0$ in $L^2(\Theta)$ and, for every $\psi \in L^2(0,T;V)$,

$$\begin{aligned} \int_0^T \langle \partial_t\varphi(t), \psi(t)\rangle_{V',V}\, dt \;&+\; \alpha \int_0^T \int_\Theta \Delta\varphi(x,t)\,\Delta\psi(x,t)\,dx\,dt \\ &+\; \int_0^T \int_\Theta (\mathbf{m}(x,t)\cdot\nabla\varphi(x,t))\,\psi(x,t)\,dx\,dt \\ &+\; a\int_0^T \int_\Theta \varphi(x,t)\,\psi(x,t)\,dx\,dt \\ &=\; \int_0^T \int_\Theta g(x,t)\,\psi(x,t)\,dx\,dt. \end{aligned}$$

Moreover, assume that $\mathbf{m} \in L^\infty(0,T;L^2(\Theta)^q)$.

Lemma 2.1. *There exists a constant $C > 0$, depending only on α, a, T, and $\|\mathbf{m}\|_{L^\infty(0,T;L^2(\Theta)^q)}$, such that for every $t \in [0,T]$,*

$$\|\varphi(t)\|^2_{L^2(\Theta)} + \alpha \int_0^t \|\Delta\varphi(s)\|^2_{L^2(\Theta)}\, ds \le C\left(\|\varphi_0\|^2_{L^2(\Theta)} + \int_0^t \|g(s)\|^2_{L^2(\Theta)}\, ds\right).$$

Proof. Multiplying (2.1) by $\varphi(t)$ and integrating with Θ, we obtain

$$\begin{aligned}\frac{1}{2}\frac{d}{dt}\|\varphi(t)\|^2_{L^2(\Theta)} &+ \alpha\|\Delta\varphi(t)\|^2_{L^2(\Theta)}\\ &+ a\|\varphi(t)\|^2_{L^2(\Theta)}\\ &= \int_\Theta g(x,t)\,\varphi(x,t)\,dx\\ &+ \int_\Theta (\mathbf{m}(x,t)\cdot\nabla\varphi(x,t))\,\varphi(x,t)\,dx.\end{aligned}$$

By Young's inequality,

$$\left|\int_\Theta g(x,t)\,\varphi(x,t)\,dx\right| \le \frac{1}{2}\|g(t)\|^2_{L^2(\Theta)} + \frac{1}{2}\|\varphi(t)\|^2_{L^2(\Theta)}.$$

Moreover, by Hölder's inequality,

$$\left|\int_\Theta (\mathbf{m}(x,t)\cdot\nabla\varphi(x,t))\,\varphi(x,t)\,dx\right| \le \|\mathbf{m}(t)\|_{L^2(\Theta)^q}\,\|\nabla\varphi(t)\|_{L^2(\Theta)}\,\|\varphi(t)\|_{L^2(\Theta)}.$$

Using the interpolation estimate,

$$\|\nabla\varphi(t)\|_{L^2(\Theta)} \le C\,\|\Delta\varphi(t)\|^{1/2}_{L^2(\Theta)}\,\|\varphi(t)\|^{1/2}_{L^2(\Theta)}.$$

Applying Young's inequality, we infer that

$$\left|\int_\Theta (\mathbf{m}(x,t)\cdot\nabla\varphi(x,t))\,\varphi(x,t)\,dx\right| \le \frac{\alpha}{2}\|\Delta\varphi(t)\|^2_{L^2(\Theta)} + C\|\mathbf{m}(t)\|^2_{L^2(\Theta)^q}\,\|\varphi(t)\|^2_{L^2(\Theta)}.$$

Consequently,

$$\frac{d}{dt}\|\varphi(t)\|^2_{L^2(\Theta)} + \alpha\|\Delta\varphi(t)\|^2_{L^2(\Theta)} \le C(1 + \|\mathbf{m}(t)\|^2_{L^2(\Theta)^q})\|\varphi(t)\|^2_{L^2(\Theta)} + \|g(t)\|^2_{L^2(\Theta)}.$$

Since $\mathbf{m} \in L^\infty(0,T;L^2(\Theta)^q)$, Gronwall's inequality yields the estimate. □

Remark 2.2. *The previous bound implies that φ is bounded in $L^2(0,T;H^2_0(\Theta))$. Furthermore, rewriting* (2.1) *as*

$$\partial_t\varphi = \alpha\Delta^2\varphi - \mathbf{m}\cdot\nabla\varphi - a\varphi + g,$$

we deduce that $\partial_t\varphi$ is bounded in $L^2(0,T;V')$.

Lemma 2.2. *Let $m \in \mathcal{M}$ satisfy $\|\nabla \cdot m\|_{L^\infty(D)} \le M$, and let $\varphi = \mathcal{Y}(m)$ be the weak solution of* (2.1). *We define*

$$\mathcal{K} := \Big(\|\varphi_0\|^2_{L^2(\Theta)} + \|g\|^2_{L^2(D)}\Big)^{\frac{1}{2}} \exp\Big(\frac{(1+M)T}{2}\Big).$$

Then the following estimates hold:

$$\|\varphi\|_{L^\infty(0,T;L^2(\Theta))} \le \mathcal{K},$$

$$\|\Delta\varphi\|_{L^2(0,T;L^2(\Theta))} \le \frac{1}{\sqrt{\alpha}}\,\mathcal{K},$$

and, consequently,

$$\|\varphi\|_{L^2(D)} \le T^{\frac{1}{2}}\,\mathcal{K}.$$

Proof. Let φ be the weak solution of (2.1) and assume that $\|\nabla \cdot m\|_{L^\infty(D)} \le M$.
For the drift term, we compute

$$\int_\Theta (m \cdot \nabla\varphi)\,\varphi\,dx = \frac{1}{2}\int_\Theta m \cdot \nabla(\varphi^2)\,dx = -\frac{1}{2}\int_\Theta (\nabla \cdot m)\,\varphi^2\,dx + \frac{1}{2}\int_{\partial\Theta} (m \cdot \nu)\,\varphi^2\,dS.$$

Since $\varphi = 0$ on $\partial\Theta$, the boundary term vanishes. Hence,

$$-\int_\Theta (m \cdot \nabla\varphi)\,\varphi\,dx = \frac{1}{2}\int_\Theta (\nabla \cdot m)\,\varphi^2\,dx \le \frac{M}{2}\|\varphi(t)\|^2_{L^2(\Theta)}.$$

Moreover, by Young's inequality,

$$\int_\Theta g(t)\,\varphi(t)\,dx \le \frac{1}{2}\|g(t)\|^2_{L^2(\Theta)} + \frac{1}{2}\|\varphi(t)\|^2_{L^2(\Theta)}.$$

Substituting the above estimates into Lemma 2.1, we obtain

$$\frac{d}{dt}\|\varphi(t)\|^2_{L^2(\Theta)} + \alpha\|\Delta\varphi(t)\|^2_{L^2(\Theta)} \le (1+M)\|\varphi(t)\|^2_{L^2(\Theta)} + \|g(t)\|^2_{L^2(\Theta)}.$$

In particular,

$$\frac{d}{dt}\|\varphi(t)\|^2_{L^2(\Theta)} \le (1+M)\|\varphi(t)\|^2_{L^2(\Theta)} + \|g(t)\|^2_{L^2(\Theta)}.$$

By Gronwall's lemma, for all $t \in [0,T]$,

$$\|\varphi(t)\|^2_{L^2(\Theta)} \le \left(\|\varphi_0\|^2_{L^2(\Theta)} + \int_0^t \|g(s)\|^2_{L^2(\Theta)}\,ds\right)\exp((1+M)t).$$

Taking the supremum over $t \in [0,T]$, we obtain

$$\|\varphi\|_{L^\infty(0,T;L^2(\Theta))} \le \Big(\|\varphi_0\|^2_{L^2(\Theta)} + \|g\|^2_{L^2(D)}\Big)^{\frac{1}{2}} \exp\Big(\tfrac{(1+M)T}{2}\Big) = \mathcal{K}.$$

Integrating the differential inequality over $(0,T)$ yields

$$\alpha\int_0^T \|\Delta\varphi(t)\|^2_{L^2(\Theta)}\,dt \le \Big(\|\varphi_0\|^2_{L^2(\Theta)} + \|g\|^2_{L^2(D)}\Big)\exp((1+M)T),$$

and therefore

$$\|\Delta\varphi\|_{L^2(0,T;L^2(\Theta))} \le \frac{1}{\sqrt{\alpha}}\,\mathcal{K}.$$

Finally,

$$\|\varphi\|_{L^2(D)} \le T^{\frac{1}{2}}\|\varphi\|_{L^\infty(0,T;L^2(\Theta))} \le T^{\frac{1}{2}}\mathcal{K}.$$

This completes the proof. □

3. Existence of a solution for the penalized problem

In order to solve the optimal control problem (2.2), we introduce a quadratic optimal control framework. The objective functional penalizes the control norm as well as the discrepancies in the final state and the final velocity. For $\gamma > 0$, we consider the following auxiliary problem associated with (2.2):

$$\begin{cases} \boldsymbol{m} \in \mathcal{M}, \\ C(\boldsymbol{m}) \leq C(\boldsymbol{h}), \forall \boldsymbol{h} \in \mathcal{M}, \end{cases} \tag{3.1}$$

where the objective functional C is given by

$$C(\boldsymbol{m}) = \frac{1}{2} \iint_D |\boldsymbol{m}|^2 dxdt + \frac{\gamma}{2} \iint_D |\varphi - \varphi_d|^2 \, dxdt, \tag{3.2}$$

and $\varphi = \varphi(t; \boldsymbol{m})$ is the state corresponding to the control $\boldsymbol{m}$. The existence and uniqueness of the weak solution $\varphi \in W(0, T)$ to system (2.1) are derived from standard arguments based on the Lax–Milgram theorem together with classical results for parabolic evolution equations [1]. We introduce the control-to-state operator

$$\mathcal{Y} : \mathcal{M} \longrightarrow W(0, T),$$

which associates to each admissible drift field $\mathbf{m} \in \mathcal{M}$ the unique solution $\varphi = \mathcal{Y}(\mathbf{m})$ of the system (2.1).

The cost functional becomes

$$C(\mathbf{m}) = \frac{1}{2} \int_0^T \int_\Theta |\mathbf{m}(x, t)|^2 \, dx \, dt + \frac{\gamma}{2} \int_0^T \int_\Theta \left| \mathcal{Y}(\mathbf{m}) - \varphi_d(x, t) \right|^2 dx \, dt,$$

where $\gamma > 0$ is a weighting parameter and $\varphi = \mathcal{Y}(\mathbf{m})$.

The first term represents the control energy, while the second term measures the tracking error over the space–time domain $D = \Theta \times (0, T)$.

Since the state equation depends bilinearly on the control through the term $\mathbf{m} \cdot \nabla\varphi$, the solution operator $\mathcal{Y}$ is nonlinear. Consequently, the associated optimal control problem is nonconvex.

Having established the well-posedness of the state system and the necessary a priori estimates, we now investigate the existence of optimal controls for the minimum energy problem. Our objective in this subsection is to prove the existence of at least one optimal drift field in the admissible set $\mathcal{M}$.

The proof is based on the direct method of calculus of variations. As a first step, we show that the cost functional C is weakly lower semicontinuous on the control set $\mathcal{M}$. This property, combined with the coercivity of C and the stability of the state equation with respect to the weak convergence of controls, allows us to conclude the existence of an optimal control.

Lemma 3.1. *The cost functional $C : \mathcal{M} \to \mathbb{R}$ defined by*

$$C(\mathbf{m}) = \frac{1}{2} \int_0^T \int_\Theta |\mathbf{m}(x, t)|^2 \, dx \, dt + \frac{\gamma}{2} \int_0^T \int_\Theta \left| \mathcal{Y}(\mathbf{m})(x, t) - \varphi_d(x, t) \right|^2 dx \, dt$$

is weakly lower semicontinuous on $\mathcal{M}$. More precisely, if

$$\mathbf{m}_n \rightharpoonup \overline{\mathbf{m}} \quad \textit{weakly in } L^2(0, T; L^2(\Theta)^q),$$

then

$$C(\overline{\mathbf{m}}) \le \liminf_{n\to\infty} C(\mathbf{m}_n).$$

Proof. Let $\{\mathbf{m}_n\} \subset \mathcal{M}$ be such that

$$\mathbf{m}_n \rightharpoonup \overline{\mathbf{m}} \quad \text{weakly in } L^2(0,T;L^2(\Theta)^q).$$

We denote by $\varphi_n = \mathcal{Y}(\mathbf{m}_n)$ the corresponding state solutions and set $\overline{\varphi} = \mathcal{Y}(\overline{\mathbf{m}})$.

The mapping

$$\mathbf{m} \mapsto \frac{1}{2}\int_0^T \int_\Theta |\mathbf{m}(x,t)|^2 \, dx\, dt$$

is convex and continuous on $L^2(0,T;L^2(\Theta)^q)$, hence it is weakly lower semicontinuous. Therefore,

$$\frac{1}{2}\int_0^T \int_\Theta |\overline{\mathbf{m}}|^2 \, dx\, dt \le \liminf_{n\to\infty} \frac{1}{2}\int_0^T \int_\Theta |\mathbf{m}_n|^2 \, dx\, dt.$$

From the uniform a priori estimates for the state equation, the sequence $\{\varphi_n\}$ is bounded in $W(0,T)$. Consequently, up to a subsequence (not relabeled),

$$\varphi_n \rightharpoonup \widetilde{\varphi} \quad \text{weakly in } L^2(0,T;H_0^2(\Theta)),$$

$$\partial_t \varphi_n \rightharpoonup \partial_t \widetilde{\varphi} \quad \text{weakly in } L^2(0,T;V').$$

Since the embedding $H_0^2(\Theta) \hookrightarrow H^1(\Theta)$ is compact, the Aubin–Lions lemma [2] yields

$$\varphi_n \to \widetilde{\varphi} \quad \text{strongly in } L^2(0,T;H^1(\Theta)),$$

and in particular,

$$\nabla\varphi_n \to \nabla\widetilde{\varphi} \quad \text{strongly in } L^2(0,T;L^2(\Theta)^q).$$

Using the weak convergence of $\mathbf{m}_n$ and the strong convergence of $\nabla\varphi_n$, we reach the limit in the bilinear term of the weak formulation. Hence, $\widetilde{\varphi}$ satisfies the state equation corresponding to the control $\overline{\mathbf{m}}$. By the uniqueness of the state solution, we conclude

$$\widetilde{\varphi} = \mathcal{Y}(\overline{\mathbf{m}}) = \overline{\varphi}.$$

Moreover,

$$\varphi_n \to \overline{\varphi} \quad \text{strongly in } L^2(D).$$

Tracking term. Since $\varphi_n \to \overline{\varphi}$ strongly in $L^2(D)$, we have

$$\int_0^T \int_\Theta \left|\varphi_n - \varphi_d\right|^2 dx\, dt \to \int_0^T \int_\Theta \left|\overline{\varphi} - \varphi_d\right|^2 dx\, dt.$$

In particular,

$$\frac{\gamma}{2}\int_0^T \int_\Theta \left|\overline{\varphi} - \varphi_d\right|^2 dx\, dt \le \liminf_{n\to\infty} \frac{\gamma}{2}\int_0^T \int_\Theta \left|\varphi_n - \varphi_d\right|^2 dx\, dt.$$

Combining the estimates for the two terms yields

$$C(\overline{\mathbf{m}}) \le \liminf_{n\to\infty} C(\mathbf{m}_n),$$

which completes the proof. □

We are now prepared to establish the existence of an optimal control for the penalized problem (3.1). More precisely, we prove that there exists at least one drift field $\mathbf{m}^* \in \mathcal{M}$ such that

$$C(\mathbf{m}^*) = \inf_{\mathbf{m}\in\mathcal{M}} C(\mathbf{m}).$$

Theorem 3.1. *There exists at least one optimal drift field $\mathbf{m}^* \in \mathcal{M}$ such that*

$$C(\mathbf{m}^*) = \min_{\mathbf{m}\in\mathcal{M}} C(\mathbf{m}).$$

Equivalently,

$$C(\mathbf{m}^*) \le C(\mathbf{m}) \quad \textit{for all } \mathbf{m} \in \mathcal{M}.$$

Proof. Since $C(\mathbf{m}) \ge 0$ for all $\mathbf{m} \in \mathcal{M}$, the quantity

$$c := \inf_{\mathbf{m}\in\mathcal{M}} C(\mathbf{m})$$

is well-defined and finite. By definition of the infimum, there exists a minimizing sequence $\{\mathbf{m}_n\} \subset \mathcal{M}$ such that

$$C(\mathbf{m}_n) \longrightarrow c \quad \text{as } n \to \infty.$$

From the definition of the cost functional, we have

$$\frac{1}{2}\int_0^T \int_\Theta |\mathbf{m}_n(x,t)|^2 \, dx\, dt \le C(\mathbf{m}_n),$$

which shows that the sequence $\{\mathbf{m}_n\}$ is bounded in $L^2(0,T;L^2(\Theta)^q)$. Consequently, there exist a subsequence, still denoted by $\{\mathbf{m}_n\}$, and an element $\mathbf{m}^* \in L^2(0,T;L^2(\Theta)^q)$ such that

$$\mathbf{m}_n \rightharpoonup \mathbf{m}^* \quad \text{weakly in } L^2(0,T;L^2(\Theta)^q).$$

Since $\mathcal{M}$ is assumed to be weakly closed, it follows that $\mathbf{m}^* \in \mathcal{M}$. Moreover, by the weak lower semicontinuity of the functional C, we obtain

$$C(\mathbf{m}^*) \le \liminf_{n\to\infty} C(\mathbf{m}_n) = c.$$

By the definition of c, we also have $c \le C(\mathbf{m}^*)$, and therefore

$$C(\mathbf{m}^*) = c.$$

This shows that $\mathbf{m}^*$ is an optimal control. □

4. Characterization of the optimal control

Let $\widehat{C}(\mathbf{m})$ denote the reduced cost functional associated with the control problem. If $\mathbf{m}^* \in \mathcal{M}$ is an optimal drift field, then it satisfies the first-order necessary optimality condition

$$D\widehat{C}(\mathbf{m}^*) = 0 \quad \text{in } L^2(Q)^q,$$

in the unconstrained case.

In order to derive an explicit expression of this condition, we compute the Gâteaux derivative of $\widehat{C}$ at an arbitrary control $\mathbf{m}$ in the direction $\mathbf{h} \in L^2(Q)^q$. This computation naturally leads to the introduction of the adjoint system and yields a characterization of the optimal drift, which will be essential for the analysis developed in the following sections.

However, under additional structural assumptions, the uniqueness of the optimal control can be established. Such conditions will be specified and discussed in a subsequent subsection.

Theorem 4.1. *Let $m \in \mathcal{M}$ be an optimal drift field for the control problem (3.1). Then m satisfies the following optimality condition:*

$$\iint_D (m - \phi\nabla\varphi) \cdot h \, dx \, dt = 0, \qquad \forall\, h \in L^2(D)^q,$$

where φ and ϕ are obtained from m as unique weak solutions of the following systems.

State equation

$$\begin{cases} \dfrac{\partial\varphi}{\partial t} - \alpha\Delta^2\varphi + m \cdot \nabla\varphi + a\varphi = g & \text{in } D = \Theta \times (0,T), \\ \varphi(x,0) = \varphi_0 & \text{in } \Theta, \\ \varphi(x,t) = \dfrac{\partial\varphi(x,t)}{\partial\nu} = 0 & \text{on } \vartheta = \partial\Theta \times (0,T). \end{cases} \tag{4.1}$$

Adjoint equation

$$\begin{cases} -\dfrac{\partial\phi}{\partial t} - \alpha\Delta^2\phi - m \cdot \nabla\phi + a\phi = \gamma(\varphi - \varphi_d) & \text{in } D, \\ \phi(x,T) = 0 & \text{in } \Theta, \\ \phi(x,t) = \dfrac{\partial\phi(x,t)}{\partial\nu} = 0 & \text{on } \vartheta. \end{cases} \tag{4.2}$$

Proof. Let $m^* \in \mathcal{M}$ be an optimal drift field and let $\varphi^* = \mathcal{Y}(m^*)$ be the corresponding state solving (2.1). We fix an arbitrary $\tilde{m} \in \mathcal{M}$ and set

$$h := \tilde{m} - m^*.$$

Since $\mathcal{M}$ is convex, for every $\varepsilon \in [0,1]$, perturbed control

$$m^\varepsilon = m^* + \varepsilon h = (1-\varepsilon)m^* + \varepsilon\tilde{m} \in \mathcal{M}$$

is admissible. We denote $\varphi^\varepsilon := \mathcal{Y}(m^\varepsilon)$.

We define the increment quotient

$$w^\varepsilon := \frac{\varphi^\varepsilon - \varphi^*}{\varepsilon}.$$

By the standard stability of the state equation and the bilinear structure of the drift term [1], w^ε converges to a function $w \in W(0,T)$, which solves the linearized system

$$\begin{cases} \dfrac{\partial w}{\partial t} - \alpha\Delta^2 w + m^* \cdot \nabla w + aw = -h \cdot \nabla\varphi^* & \text{in } D, \\ w(x,0) = 0 & \text{in } \Theta, \\ w = \dfrac{\partial w}{\partial\nu} = 0 & \text{on } \vartheta. \end{cases}$$

Recall that

$$\widehat{C}(m) = \frac{1}{2}\iint_D |m|^2\,dx\,dt + \frac{\gamma}{2}\iint_D |\mathcal{Y}(m) - \varphi_d|^2\,dx\,dt.$$

A direct computation yields

$$\begin{aligned}\frac{\widehat{C}(m^\varepsilon) - \widehat{C}(m^*)}{\varepsilon} &= \iint_D m^* \cdot h\,dx\,dt + \gamma\iint_D (\varphi^* - \varphi_d)\,w^\varepsilon\,dx\,dt + \frac{\varepsilon}{2}\iint_D |h|^2\,dx\,dt \\ &+ \frac{\gamma\varepsilon}{2}\iint_D |w^\varepsilon|^2\,dx\,dt.\end{aligned}$$

Letting $\varepsilon \to 0$, we obtain

$$D\widehat{C}(m^*)\,h = \iint_D m^* \cdot h\,dx\,dt + \gamma\iint_D (\varphi^* - \varphi_d)\,w\,dx\,dt.$$

Let ϕ be the solution of the adjoint problem

$$\begin{cases} -\dfrac{\partial\phi}{\partial t} - \alpha\Delta^2\phi - m^* \cdot \nabla\phi + a\phi = \gamma(\varphi^* - \varphi_d) & \text{in } D, \\ \phi(x,T) = 0 & \text{in } \Theta, \\ \phi = \dfrac{\partial\phi}{\partial\nu} = 0 & \text{on } \vartheta. \end{cases}$$

Multiplying the linearized equation by ϕ, integrating over D, and performing integration by parts in time and space, we obtain

$$\gamma\iint_D (\varphi^* - \varphi_d)\,w\,dx\,dt = -\iint_D (h \cdot \nabla\varphi^*)\,\phi\,dx\,dt = -\iint_D (\phi\nabla\varphi^*) \cdot h\,dx\,dt.$$

Substituting the previous identity into the expression of $D\widehat{C}(m^*)\,h$ yields

$$D\widehat{C}(m^*)\,h = \iint_D (m^* - \phi\nabla\varphi^*) \cdot h\,dx\,dt.$$

Since m^* is optimal and $m^\varepsilon \in \mathcal{M}$, we have

$$0 \le \frac{\widehat{C}(m^\varepsilon) - \widehat{C}(m^*)}{\varepsilon} \quad \text{for all } \varepsilon \in (0,1].$$

Letting $\varepsilon \to 0$ gives

$$D\widehat{C}(m^*)\,h \ge 0.$$

Hence,

$$\iint_D (m^* - \phi\nabla\varphi^*) \cdot (\tilde{m} - m^*)\,dx\,dt \ge 0, \qquad \forall\, \tilde{m} \in \mathcal{M}.$$

In the unconstrained case $\mathcal{M} = L^2(D)^q$, this reduces to

$$\iint_D (m^* - \phi\nabla\varphi^*) \cdot h\,dx\,dt = 0, \qquad \forall\, h \in L^2(D)^q. \tag{4.3}$$

□

Corollary 4.1. *Assume that the optimal drift field has the form*

$$m^*(x,t) = v^*(t)\mathbb{1}_\omega(x) \quad \text{a.e. in } D,$$

where $v^* \in L^2(0,T;\mathbb{R}^q)$ and $\omega \subset \Theta$ denotes the actuator region with $\mu(\omega) > 0$. Then v^* satisfies, for a.e. $t \in (0,T)$,

$$v^*(t) = \frac{1}{\mu(\omega)} \int_\omega \phi(x,t)\, \nabla\varphi^*(x,t)\, dx.$$

Corollary 4.2. *If $\mathcal{M} = L^\infty(0,T;L^2(\Theta)^q)$, then*

$$\mathbf{m}^* = \phi^* \nabla\varphi^* \quad \text{a.e. in } D,$$

and if $\mathcal{M}$ is defined by box constraints $\mathbf{m}_a \le \mathbf{m} \le \mathbf{m}_b$ a.e. in D, then

$$\mathbf{m}^*(x,t) = \mathbf{P}_{[\mathbf{m}_a(x,t),\, \mathbf{m}_b(x,t)]}\big(\phi(x,t)\nabla\varphi^*(x,t)\big),$$

where $\mathbf{P}$ denotes the componentwise projection.

Let $m \in \mathcal{M}$ and let $\varphi = \mathcal{Y}(m)$ be the corresponding state that solves (2.1). Let ϕ be the unique weak solution of the adjoint problem (4.2), and then the following estimates hold:

Lemma 4.1. *Let $m \in \mathcal{M}$ satisfy $\|\nabla \cdot m\|_{L^\infty(D)} \le M$, and let $a > 0$ be a constant. Let ϕ be the weak solution of the adjoint problem* (4.2)*. We define*

$$\mathcal{K}_\phi := \gamma^{\frac{1}{2}}\, \|\varphi - \varphi_d\|_{L^2(D)} \exp\Big(\frac{(1+M)T}{2}\Big),$$

and then the following estimates hold:

$$\|\phi\|_{L^\infty(0,T;L^2(\Theta))} \le \mathcal{K}_\phi,$$

$$\|\Delta\phi\|_{L^2(0,T;L^2(\Theta))} \le \frac{1}{\sqrt{\alpha}}\, \mathcal{K}_\phi,$$

and, consequently,

$$\|\phi\|_{L^2(D)} \le T^{\frac{1}{2}}\, \mathcal{K}_\phi.$$

Proof. The proof follows from standard energy estimates for linear fourth-order parabolic equations (see Lemma 2.2). For similar arguments in the context of parabolic optimal control problems, we refer to Lions [1] and Tröltzsch [5]. The extension to the present fourth-order operator is straightforward. □

We emphasize that the uniqueness of the optimal control cannot, in general, be guaranteed. Indeed, due to the bilinear coupling between the state and the control through the term $\mathbf{m} \cdot \nabla\varphi$, the control-to-state operator $\mathcal{Y}$ is nonlinear. Consequently, the cost functional C is typically nonconvex and multiple (possibly local) minimizers may exist.

Theorem 4.2. *Assume that $a > 0$ is a constant and that $m \in \mathcal{M}$ satisfies $\|\nabla \cdot m\|_{L^\infty(D)} \le M$. Let $\varphi_0 \in L^2(\Theta)$, $g \in L^2(D)$, and $\varphi_d \in L^2(D)$.*

Define

$$\mathcal{K} = \Big(\|\varphi_0\|^2_{L^2(\Theta)} + \|g\|^2_{L^2(D)}\Big)^{\frac{1}{2}} \exp\Big(\frac{(1+M)T}{2}\Big),$$

and

$$\mathcal{K}_\phi = \gamma^{\frac{1}{2}}\Big(T^{\frac{1}{2}}\mathcal{K} + \|\varphi_d\|_{L^2(D)}\Big)\exp\Big(\frac{(1+M)T}{2}\Big).$$

If the following smallness condition holds:

$$\Big[2\mathcal{K}\mathcal{K}_\phi + \gamma\mathcal{K}^2\Big] < 1, \tag{4.4}$$

then the optimal control is unique in $\mathcal{M}$.

Proof. Let m_1, m_2 be two optimal controls in $\mathcal{M}$, and let (φ_1, ϕ_1) and (φ_2, ϕ_2) be the corresponding state–adjoint pairs, where φ_i solves (2.1) with $m = m_i$ and ϕ_i solves (4.2) with $\varphi = \varphi_i$ $(i = 1, 2)$. We set

$$w := \varphi_1 - \varphi_2, \qquad z := \phi_1 - \phi_2, \qquad \delta m := m_1 - m_2.$$

Subtracting the two state equations yields

$$\partial_t w - \alpha\Delta^2 w + m_1 \cdot \nabla w + aw = -\delta m \cdot \nabla\varphi_2 \quad \text{in } D, \qquad w(\cdot, 0) = 0,$$

with the same boundary conditions as in (2.1). Applying the estimate of Lemma 2.2 to the above equation, we obtain

$$\|w\|_{L^2(0,T;H^2_0(\Theta))} \le \|\delta m \cdot \nabla\varphi_2\|_{L^2(0,T;H^{-2}(\Theta))}.$$

Using the product estimate $\|\delta m \cdot \nabla\varphi_2\|_{H^{-2}(\Theta)} \le \|\delta m\|\,\|\varphi_2\|_{L^2(\Theta)}$, we get

$$\|w\|_{L^2(0,T;H^2_0(\Theta))} \le \|\delta m\|_{\mathcal{M}}\,\|\varphi_2\|_{L^\infty(0,T;L^2(\Theta))} \le \mathcal{K}\,\|\delta m\|_{\mathcal{M}}. \tag{4.5}$$

Subtracting the adjoint equations (4.2) satisfied by ϕ_1 and ϕ_2 gives

$$-\partial_t z - \alpha\Delta^2 z - m_1 \cdot \nabla z + az = -\delta m \cdot \nabla\phi_2 + \gamma w \quad \text{in } D, \qquad z(\cdot, T) = 0,$$

with the same boundary conditions as in (4.2). Applying Lemma 4.1 to this equation yields

$$\|z\|_{L^2(0,T;H^2_0(\Theta))} \le \|\delta m \cdot \nabla\phi_2\|_{L^2(0,T;H^{-2}(\Theta))} + \gamma\|w\|_{L^2(0,T;H^2_0(\Theta))}.$$

Using again the product estimate $\|\delta m \cdot \nabla\phi_2\|_{H^{-2}(\Theta)} \le \|\delta m\|\,\|\phi_2\|_{L^2(\Theta)}$, and the bounds $\|\phi_2\|_{L^\infty(0,T;L^2(\Theta))} \le \mathcal{K}_\phi$ and (4.5), we obtain

$$\|z\|_{L^2(0,T;H^2_0(\Theta))} \le \Big(\mathcal{K}_\phi + \gamma\mathcal{K}\Big)\,\|\delta m\|_{\mathcal{M}}. \tag{4.6}$$

From the first-order optimality condition,

$$m_i = \phi_i\,\nabla\varphi_i \qquad \text{a.e. in } D, \quad i = 1, 2,$$

we have

$$\delta m = (\phi_1\nabla\varphi_1 - \phi_2\nabla\varphi_2) = \Big(z\,\nabla\varphi_1 + \phi_2\,\nabla w\Big).$$

Therefore,

$$\|\delta m\|_{\mathcal{M}} \leq \Big[\|w\|_{L^2(0,T;H_0^2(\Theta))}\|\phi_1\|_{L^\infty(0,T;L^2(\Theta))} + \|z\|_{L^2(0,T;H_0^2(\Theta))}\|\varphi_2\|_{L^\infty(0,T;L^2(\Theta))}\Big].$$

Using estimates $\|\phi_1\|_{L^\infty(0,T;L^2(\Theta))} \leq \mathcal{K}_\phi$, $\|\varphi_2\|_{L^\infty(0,T;L^2(\Theta))} \leq \mathcal{K}$, together with (4.5) and (4.6), we deduce

$$\|\delta m\|_{\mathcal{M}} \leq \Big[\mathcal{K}\mathcal{K}_\phi + \mathcal{K}(\mathcal{K}_\phi + \gamma\mathcal{K})\Big]\|\delta m\|_{\mathcal{M}} = \Big[2\mathcal{K}\mathcal{K}_\phi + \gamma\mathcal{K}^2\Big]\|\delta m\|_{\mathcal{M}}.$$

If the smallness condition (4.4) holds, then necessarily $\|\delta m\|_{\mathcal{M}} = 0$, hence $m_1 = m_2$ a.e. in D. This shows the uniqueness of the optimal control.

Remark 4.1. *The optimal control problem considered in this work involves several specific difficulties:*

1. *The fourth-order nature of the state equation requires more delicate a priori estimates and regularity arguments than in the case of classical second-order reaction–diffusion systems.*
2. *The bilinear drift control introduces a nonlinear coupling between the state and the control, which complicates both the analysis of the state system and the derivation of the corresponding optimality conditions.*
3. *The minimum-energy formulation studied here is more subtle than the standard tracking-type problem, since the control must be characterized through a limiting procedure based on a family of penalized problems.*

These aspects make the present framework substantially different from, and analytically more delicate than, many existing results in the literature on lower-order optimal control problems.

□

5. Limit minimum-energy control problem

The main goal of this section is to propose a method to solve the problem 2.2. To realize this goal, we consider a family $C_\epsilon(m)$ of the penalized problem 3.1, given by

$$C_\epsilon(\boldsymbol{m_\epsilon}) = \frac{\epsilon}{2}\iint_D |\boldsymbol{m_\epsilon}|^2 dxdt + \frac{\gamma}{2}\iint_D |\varphi_\epsilon - \varphi_d|^2\, dxdt, \tag{5.1}$$

and its minimum using Theorem 4.1 to verify

$$\iint_D (m_\epsilon - \frac{1}{\epsilon}\phi_\epsilon\nabla\varphi_\epsilon)\cdot h\, dx\, dt = 0, \qquad \forall\, h \in L^2(D)^q.$$

Proposition 5.1. *For every $\varepsilon > 0$, let $\boldsymbol{m}_\varepsilon$ be an optimal control of* (5.2) *with associated state $\varphi_\varepsilon := \mathcal{Y}(\boldsymbol{m}_\varepsilon)$. We define*

$$E_\varepsilon = \frac{1}{2}\iint_D |\boldsymbol{m}_\varepsilon|^2\, dxdt, \qquad J_\varepsilon = \frac{\gamma}{2}\iint_D |\varphi_\varepsilon - \varphi_d|^2\, dxdt, \qquad C_\varepsilon = C_\varepsilon(\boldsymbol{m}_\varepsilon) = \varepsilon E_\varepsilon + J_\varepsilon,$$

and then, for any $0 < \varepsilon_1 < \varepsilon_2$, the following properties hold:

1. *$C_{\varepsilon_1} \leq C_{\varepsilon_2}$, i.e., the optimal value C_ε is nonincreasing as $\varepsilon \to 0$.*

2. $E_{\varepsilon_1} \geq E_{\varepsilon_2}$, *i.e., the energy* $\iint_D |\boldsymbol{m}_\varepsilon|^2$ *does not decrease as* $\varepsilon \to 0$.
3. $J_{\varepsilon_1} \leq J_{\varepsilon_2}$, *i.e., the tracking term* $\iint_D |\varphi_\varepsilon - \varphi_d|^2$ *is not increasing as* $\varepsilon \to 0$. *In particular,* $(\varphi_\varepsilon - \varphi_d)_{\varepsilon>0}$ *is bounded in* $L^2(D)$*; therefore, there exists a sequence* $\varepsilon_k \downarrow 0$ *and* $\eta \in L^2(D)$ *such that*

$$\varphi_{\varepsilon_k} - \varphi_d \rightharpoonup \eta \quad \text{weakly in } L^2(D).$$

Proof. Let $0 < \varepsilon_1 < \varepsilon_2$. By the optimality of $\boldsymbol{m}_{\varepsilon_1}$ for C_{ε_1} and of $\boldsymbol{m}_{\varepsilon_2}$ for C_{ε_2}, we have

$$C_{\varepsilon_1}(\boldsymbol{m}_{\varepsilon_1}) \leq C_{\varepsilon_1}(\boldsymbol{m}_{\varepsilon_2}), \qquad C_{\varepsilon_2}(\boldsymbol{m}_{\varepsilon_2}) \leq C_{\varepsilon_2}(\boldsymbol{m}_{\varepsilon_1}).$$

Writing these inequalities in terms of E_ε and J_ε gives

$$\varepsilon_1 E_{\varepsilon_1} + J_{\varepsilon_1} \leq \varepsilon_1 E_{\varepsilon_2} + J_{\varepsilon_2}, \qquad \varepsilon_2 E_{\varepsilon_2} + J_{\varepsilon_2} \leq \varepsilon_2 E_{\varepsilon_1} + J_{\varepsilon_1}.$$

Adding the two inequalities yields

$$(\varepsilon_2 - \varepsilon_1)(E_{\varepsilon_2} - E_{\varepsilon_1}) \leq 0,$$

hence $E_{\varepsilon_1} \geq E_{\varepsilon_2}$, which proves 2.

Next, from

$$\varepsilon_1 E_{\varepsilon_1} + J_{\varepsilon_1} \leq \varepsilon_1 E_{\varepsilon_2} + J_{\varepsilon_2}$$

and $E_{\varepsilon_1} \geq E_{\varepsilon_2}$, we obtain $J_{\varepsilon_1} \leq J_{\varepsilon_2}$, proving 3.

Finally, using

$$C_{\varepsilon_2}(\boldsymbol{m}_{\varepsilon_2}) \leq C_{\varepsilon_2}(\boldsymbol{m}_{\varepsilon_1})$$

and $E_{\varepsilon_1} \geq E_{\varepsilon_2}$, we get $C_{\varepsilon_1} \leq C_{\varepsilon_2}$, proving 1.

The boundedness of $(\varphi_\varepsilon - \varphi_d)$ in $L^2(D)$ follows directly from 3, and the weak convergence statement is a consequence of the Banach–Alaoglu theorem; see [7]. □

We are now in a position to state the main theorem concerning the solution of the proposed minimum energy control problem (2.2).

Theorem 5.1. *For each* $\varepsilon > 0$, *let* $\boldsymbol{m}_\varepsilon \in \mathcal{M}$ *be an optimal control minimizing*

$$C_\varepsilon(\boldsymbol{m}) = \frac{\varepsilon}{2} \iint_D |\boldsymbol{m}|^2 \, dxdt + \frac{\gamma}{2} \iint_D |\varphi - \varphi_d|^2 \, dxdt, \tag{5.2}$$

and let $\varphi_\varepsilon = \mathcal{Y}(\boldsymbol{m}_\varepsilon)$ *be the associated state.*

Then there exist a sequence $\varepsilon_k \downarrow 0$, *a control* $\boldsymbol{m}_0 \in L^2(D)^q$, *and a function* $\varphi_0 \in L^2(D)$ *such that:*

1. $\boldsymbol{m}_{\varepsilon_k} \rightharpoonup \boldsymbol{m}_0$ *weakly in* $L^2(D)^q$, *and* $\varphi_{\varepsilon_k} \rightharpoonup \varphi_0$ *weakly in* $L^2(D)$, *where* $\varphi_0 = \mathcal{Y}(\boldsymbol{m}_0)$.
2. $\boldsymbol{m}_0$ *minimizes the tracking functional*

$$J_0(\boldsymbol{m}) := \frac{\gamma}{2} \iint_D |\mathcal{Y}(\boldsymbol{m}) - \varphi_d|^2 \, dxdt$$

over $\mathcal{M}$, *that is,*

$$J_0(\boldsymbol{m}_0) = \inf_{\boldsymbol{m} \in \mathcal{M}} J_0(\boldsymbol{m}).$$

3. Let

$$\mathcal{U}^* := \arg\min_{\boldsymbol{m}\in\mathcal{M}} J_0(\boldsymbol{m}).$$

Then $\boldsymbol{m}_0$ is a minimum-energy element of $\mathcal{U}^*$, namely,

$$\iint_D |\boldsymbol{m}_0|^2\,dxdt \le \iint_D |\boldsymbol{m}|^2\,dxdt, \qquad \forall\, \boldsymbol{m}\in\mathcal{U}^*.$$

Equivalently, $\boldsymbol{m}_0$ solves the minimum-energy problem

$$\begin{cases} \textbf{min} & \displaystyle\iint_D |\boldsymbol{m}|^2\,dxdt, \\ \textit{subject to} & \boldsymbol{m}\in\mathcal{U}^*. \end{cases} \tag{5.3}$$

Proof. Let $\varepsilon_0 > 0$ be fixed. By Proposition 5.1, the map $\varepsilon \mapsto C_\varepsilon(\boldsymbol{m}_\varepsilon)$ does not increase as $\varepsilon \to 0$. Hence, for all $0 < \varepsilon \le \varepsilon_0$,

$$C_\varepsilon(\boldsymbol{m}_\varepsilon) \le C_{\varepsilon_0}(\boldsymbol{m}_{\varepsilon_0}) = \overline{C}. \tag{5.4}$$

Moreover, by Proposition 5.1, the tracking term is bounded:

$$J_\varepsilon = \frac{\gamma}{2}\iint_D |\varphi_\varepsilon - \varphi_d|^2\,dxdt \le J_{\varepsilon_0} =: \overline{J}. \tag{5.5}$$

Since $C_\varepsilon = \varepsilon E_\varepsilon + J_\varepsilon$ and $J_\varepsilon \ge 0$, from (5.4), we get $\varepsilon E_\varepsilon \le \overline{C}$, i.e.,

$$\frac{\varepsilon}{2}\|\boldsymbol{m}_\varepsilon\|^2_{L^2(D)^q} \le \overline{C}, \qquad 0 < \varepsilon \le \varepsilon_0.$$

In particular, choosing a sequence $\varepsilon_k \downarrow 0$ such that $\|\boldsymbol{m}_{\varepsilon_k}\|_{L^2(D)^q}$ is bounded (for instance, take any sequence $\varepsilon_k \downarrow 0$ with $\varepsilon_k \ge \varepsilon_0/2$ for finitely many initial indices), we obtain that $(\boldsymbol{m}_{\varepsilon_k})$ is bounded in $L^2(D)^q$. Hence, by the Banach–Alaoglu theorem [7], there exists a subsequence (not relabeled) and $\boldsymbol{m}_0 \in L^2(D)^q$ such that

$$\boldsymbol{m}_{\varepsilon_k} \rightharpoonup \boldsymbol{m}_0 \quad \text{weakly in } L^2(D)^q. \tag{5.6}$$

Also, by (5.5), $(\varphi_{\varepsilon_k} - \varphi_d)$ is bounded in $L^2(D)$, hence $(\varphi_{\varepsilon_k})$ is bounded in $L^2(D)$ and there exists $\varphi_0 \in L^2(D)$ such that

$$\varphi_{\varepsilon_k} \rightharpoonup \varphi_0 \quad \text{weakly in } L^2(D). \tag{5.7}$$

Passing to the limit in the state equation (using the linearity/continuity of the control-to-state map), we obtain $\varphi_0 = \mathcal{Y}(\boldsymbol{m}_0)$. This proves 1.

Let $\boldsymbol{m}\in\mathcal{M}$ be arbitrary and set $\varphi = \mathcal{Y}(\boldsymbol{m})$. By the optimality of $\boldsymbol{m}_\varepsilon$ for C_ε,

$$\frac{\varepsilon}{2}\|\boldsymbol{m}_\varepsilon\|^2_{L^2(D)^q} + \frac{\gamma}{2}\|\varphi_\varepsilon - \varphi_d\|^2_{L^2(D)} \le \frac{\varepsilon}{2}\|\boldsymbol{m}\|^2_{L^2(D)^q} + \frac{\gamma}{2}\|\varphi - \varphi_d\|^2_{L^2(D)}.$$

The removal of the nonnegative term $\frac{\varepsilon}{2}\|\boldsymbol{m}_\varepsilon\|^2$ yields

$$J_0(\boldsymbol{m}_\varepsilon) \le J_0(\boldsymbol{m}) + \frac{\varepsilon}{2}\|\boldsymbol{m}\|^2_{L^2(D)^q}.$$

Letting $\varepsilon = \varepsilon_k \to 0$ gives

$$\limsup_{k\to\infty} J_0(\boldsymbol{m}_{\varepsilon_k}) \le J_0(\boldsymbol{m}), \qquad \forall\, \boldsymbol{m} \in \mathcal{M}.$$

On the other hand, since $\varphi_{\varepsilon_k} = \mathcal{Y}(\boldsymbol{m}_{\varepsilon_k})$ and $\varphi_0 = \mathcal{Y}(\boldsymbol{m}_0)$, the weak lower semicontinuity of the L^2-norm implies

$$J_0(\boldsymbol{m}_0) = \frac{\gamma}{2}\|\varphi_0 - \varphi_d\|^2_{L^2(D)} \le \liminf_{k\to\infty} \frac{\gamma}{2}\|\varphi_{\varepsilon_k} - \varphi_d\|^2_{L^2(D)} = \liminf_{k\to\infty} J_0(\boldsymbol{m}_{\varepsilon_k}).$$

Combining the last two inequalities yields

$$J_0(\boldsymbol{m}_0) \le J_0(\boldsymbol{m}), \qquad \forall\, \boldsymbol{m} \in \mathcal{M},$$

which proves 2.

Let $\boldsymbol{m} \in \mathcal{U}^*$, i.e., $J_0(\boldsymbol{m}) = \inf_{\mathcal{M}} J_0$. From the optimality inequality,

$$\frac{\varepsilon}{2}\|\boldsymbol{m}_\varepsilon\|^2_{L^2(D)^q} + J_0(\boldsymbol{m}_\varepsilon) \le \frac{\varepsilon}{2}\|\boldsymbol{m}\|^2_{L^2(D)^q} + J_0(\boldsymbol{m}).$$

Using $J_0(\boldsymbol{m}) \le J_0(\boldsymbol{m}_\varepsilon)$, we obtain

$$\frac{\varepsilon}{2}\|\boldsymbol{m}_\varepsilon\|^2_{L^2(D)^q} \le \frac{\varepsilon}{2}\|\boldsymbol{m}\|^2_{L^2(D)^q}, \qquad \forall\, \varepsilon > 0,$$

hence $\|\boldsymbol{m}_\varepsilon\|_{L^2(D)^q} \le \|\boldsymbol{m}\|_{L^2(D)^q}$ for all $\varepsilon > 0$. Passing to the limit along ε_k and using weak lower semicontinuity, we get

$$\|\boldsymbol{m}_0\|^2_{L^2(D)^q} \le \liminf_{k\to\infty} \|\boldsymbol{m}_{\varepsilon_k}\|^2_{L^2(D)^q} \le \|\boldsymbol{m}\|^2_{L^2(D)^q}, \qquad \forall\, \boldsymbol{m} \in \mathcal{U}^*,$$

which proves 3. □

The penalized functional C_ε introduces a regularization term $\varepsilon\|\boldsymbol{m}\|^2_{L^2(D)^q}$ that ensures the existence and stability of optimal controls for each $\varepsilon > 0$. As $\varepsilon \to 0$, this penalization vanishes and the sequence of optimal controls $(\boldsymbol{m}_\varepsilon)$ converges (up to a subsequence) toward a control solving the unregularized tracking problem. Moreover, the limit control is selected as the element of minimal L^2-energy among all minimizers of the tracking functional. Therefore, penalized problems provide a natural approximation of the minimum-energy control problem (2.2).

6. Numerical approach using the conjugate gradient method

In this section, we propose a numerical method for approximating the solution of the optimal control problem introduced previously. The proposed approach is based on a conjugate gradient (CG) method applied to the reduced cost functional.

The main idea consists of iteratively updating the control variable using the gradient of the objective functional. This gradient is obtained from the optimality system derived in the previous section. More precisely, for a given control, the state equation is first solved forward in time and then the corresponding adjoint equation is solved backward in time. These two solutions allow the computation of the gradient of the reduced functional.

Starting from an initial admissible control, the algorithm generates a sequence of controls by moving along conjugate descent directions. At each iteration, a suitable stepsize is computed in order to decrease the value of the cost functional. To reduce the computational cost, an approximate stepsize based on a quadratic approximation of the functional is employed instead of solving an exact minimization problem.

The iterative process is repeated until a prescribed stopping criterion is satisfied, typically when the norm of the gradient becomes sufficiently small.

It should be noted that each iteration of the proposed algorithm requires solving only the state system and the adjoint system, which makes the method simple and computationally efficient for the control problem considered.

In this section, we propose a numerical method for approximating the solution of the proposed minimum-energy optimal control problem 2.2. The method is based on a conjugate gradient algorithm applied to the penalized cost functional C_ε.

6.1. Computation of the gradient

Let $\boldsymbol{m} \in \mathcal{M}$ be an admissible control, and let $\varphi = \mathcal{Y}(\boldsymbol{m})$ denote the associated solution of the state system (2.1).

Let $\boldsymbol{h} \in \mathcal{M}$ be an arbitrary perturbation direction and we define the perturbed control

$$\boldsymbol{m}_\theta = \boldsymbol{m} + \theta \boldsymbol{h}, \qquad \theta > 0.$$

We denote by φ_θ the corresponding state solution.

Setting

$$w = \left.\frac{d\varphi_\theta}{d\theta}\right|_{\theta=0},$$

the function w satisfies the linearized system

$$\begin{cases} \dfrac{\partial w}{\partial t} - \alpha\Delta^2 w + m \cdot \nabla w + aw = -\boldsymbol{h} \cdot \nabla\varphi & \text{in } D, \\ w(x,0) = 0 & \text{in } \Theta, \\ w = \dfrac{\partial w}{\partial \nu} = 0 & \text{on } \vartheta. \end{cases}$$

The penalized cost functional is defined by

$$C_\varepsilon(\boldsymbol{m}) = \frac{\varepsilon}{2}\iint_D |\boldsymbol{m}|^2\, dxdt + \frac{\gamma}{2}\iint_D |\varphi - \varphi_d|^2\, dxdt.$$

Its directional derivative in the direction $\boldsymbol{h}$ is given by

$$DC_\varepsilon(\boldsymbol{m})\boldsymbol{h} = \varepsilon\iint_D \boldsymbol{m} \cdot \boldsymbol{h}\, dxdt + \gamma\iint_D (\varphi - \varphi_d) w\, dxdt.$$

Let ϕ be the solution of the adjoint problem (4.2). Multiplying the linearized equation by ϕ, integrating over D, and using integration by parts together with the boundary conditions, we obtain the following result.

$$\gamma\iint_D (\varphi - \varphi_d) w\, dxdt = -\iint_D (\boldsymbol{h} \cdot \nabla\varphi)\phi\, dxdt.$$

Consequently,

$$DC_\varepsilon(\boldsymbol{m})\boldsymbol{h} = \iint_D (\varepsilon \boldsymbol{m} - \phi \nabla \varphi) \cdot \boldsymbol{h}\, dxdt.$$

Hence, the gradient of the functional C_ε is

$$\nabla C_\varepsilon(\boldsymbol{m}) = \varepsilon \boldsymbol{m} - \phi \nabla \varphi.$$

6.2. Conjugate gradient algorithm

The conjugate gradient approach is adopted in this work because of its efficiency in solving large-scale optimal control problems governed by partial differential equations. In the framework considered, the gradient of the cost functional can be calculated by means of the state and adjoint systems, making the CG scheme a natural and computationally attractive choice. In addition, compared to the classical steepest descent method, the conjugate gradient algorithm generally exhibits better convergence behavior while avoiding the costly construction of second-order information [15].
Starting from an initial admissible control

$$\boldsymbol{m}_0 \in \mathcal{M},$$

the conjugate gradient method generates a sequence $(\boldsymbol{m}^k)_{k\geq 0}$ as follows.

Algorithm:

1. Solve the state equation associated with $\boldsymbol{m}^k$ and compute the state φ^k.
2. Solve the adjoint equation corresponding to φ^k and obtain ϕ^k.
3. Compute the gradient
$$\boldsymbol{g}^k = \varepsilon \boldsymbol{m}^k - \phi^k \nabla \varphi^k.$$
4. If
$$\|\boldsymbol{g}^k\|_{L^2(D)}$$
is sufficiently small, stop the iteration.
5. Define the conjugate descent direction
$$\boldsymbol{w}^k = \begin{cases} \boldsymbol{g}^k, & k = 0, \\ \boldsymbol{g}^k + \beta_k \boldsymbol{w}^{k-1}, & k \geq 1, \end{cases}$$
where
$$\beta_k = \frac{\|\boldsymbol{g}^k\|^2_{L^2(D)}}{\|\boldsymbol{g}^{k-1}\|^2_{L^2(D)}}.$$
6. Compute the stepsize $\rho_k > 0$ defined by
$$\rho_k = \arg\min_{\rho>0} C_\varepsilon(\boldsymbol{m}^k - \rho \boldsymbol{w}^k).$$
7. Update the control
$$\boldsymbol{m}^{k+1} = \boldsymbol{m}^k - \rho_k \boldsymbol{w}^k.$$

8. Set $k \leftarrow k + 1$ and repeat the procedure.

Remark 6.1. *1. Each iteration of the algorithm requires solving only one state equation and one adjoint equation. Therefore, the proposed conjugate gradient method is simple to implement and computationally efficient for the optimal control problem considered.*

2. In practice, computing the exact stepsize ρ_k by solving the minimization problem

$$\rho_k = \arg\min_{\rho>0} C_\varepsilon(\boldsymbol{m}^k - \rho \boldsymbol{w}^k)$$

is computationally expensive since each evaluation of the functional C_ε requires solving the state equation. Therefore, an approximate stepsize based on a quadratic approximation of the functional is employed. In this work, the stepsize is computed as

$$\rho_k = \frac{(\boldsymbol{g}^k, \boldsymbol{w}^k)_{L^2(D)}}{\|\boldsymbol{w}^k\|^2_{L^2(D)}},$$

which ensures a sufficient decrease in functional cost while keeping computational cost low and is widely used in conjugate gradient methods for optimal control problems [5].

In this work, the optimal control problem is approximated through the penalized functional C_ε, which combines a tracking term and a control energy term. The proposed conjugate gradient algorithm is employed to compute numerical approximations of optimal controls.

From the well-posedness of the state system and the adjoint equation, the reduced functional C_ε is continuously differentiable in $L^2(D)^q$, and its gradient is given by

$$\nabla C_\varepsilon(\boldsymbol{m}) = \varepsilon \boldsymbol{m} - \phi \nabla \varphi.$$

This explicit characterization allows for the construction of an efficient iterative optimization procedure requiring only the resolution of one state equation and one adjoint equation at each iteration.

The conjugate gradient algorithm generates a sequence of admissible controls $(\boldsymbol{m}^k)_{k\geq 0}$ that produces a monotone decrease in the cost functional. Since the functional is bounded from below, the sequence of functional values converges. Moreover, the coercivity induced by the regularization parameter $\varepsilon > 0$ guaranties the boundedness of the control sequence in $L^2(D)^q$.

The stability properties of the state and adjoint systems imply that the gradient depends continuously on the control variable. Consequently, small perturbations in the initial control or during iterations produce only small variations in the generated sequence, ensuring the stability of the proposed algorithm.

The descent property of the conjugate gradient method further implies that the norm of the gradient tends to zero along the iterations, namely,

$$\|\nabla C_\varepsilon(\boldsymbol{m}^k)\|_{L^2(D)} \longrightarrow 0, \qquad k \to \infty.$$

Hence, every accumulation point of the sequence generated by the algorithm is a stationary solution of the penalized optimal control problem.

Finally, the parameter ε plays the role of a regularization coefficient. When $\varepsilon \to 0$, the sequence of optimal controls associated with penalized problems remains bounded and admits weakly convergent

subsequences. Using the continuity of the control-to-state mapping, the corresponding states converge toward a limit state satisfying the desired tracking objective.

Therefore, the penalized formulation provides a consistent approximation of the minimum energy control problem, and the controls computed by the proposed conjugate gradient algorithm converge, as $\varepsilon \to 0$, toward a minimum energy control that achieves the best approximation of the target state.

7. Numerical experiments

7.1. Initial states and parameters

In this section, numerical simulations are performed in order to illustrate the efficiency of the proposed optimal control method. We consider the optimal control problem in the domain

$$\Theta = (0,1)^2, \quad T = 1, \quad D = \Theta \times (0,T).$$

The state equation is

$$\frac{\partial \varphi}{\partial t} - \alpha \Delta^2 \varphi + \boldsymbol{m} \cdot \nabla \varphi + a\varphi = g \quad \text{in } D,$$

with homogeneous boundary conditions;

$$\varphi = \frac{\partial \varphi}{\partial \nu} = 0 \quad \text{on } \partial\Theta \times (0,T),$$

and initial condition $\varphi(x,0) = \varphi_0(x)$. The objective functional is

$$C_\varepsilon(\boldsymbol{m}) = \frac{\varepsilon}{2} \iint_D |\boldsymbol{m}|^2 \, dxdt + \frac{\gamma}{2} \iint_D |\varphi - \varphi_d|^2 \, dxdt.$$

To evaluate the efficiency of the proposed algorithm, we construct an example with a known exact solution. We choose

$$\varphi(x,t) = e^t \sin(\pi x_1) \sin(\pi x_2),$$

and

$$\phi(x,t) = (T-t) \sin(\pi x_1) \sin(\pi x_2).$$

From the optimality condition

$$\nabla C_\varepsilon(\boldsymbol{m}) = 0,$$

we obtain

$$\boldsymbol{m}^* = \frac{1}{\varepsilon} \phi \nabla \varphi.$$

After computation,

$$\boldsymbol{m}^*(x,t) = \frac{\pi e^t (T-t)}{\varepsilon} \begin{pmatrix} \cos(\pi x_1) \sin(\pi x_2) \\ \sin(\pi x_1) \cos(\pi x_2) \end{pmatrix}.$$

The source term is defined by

$$g = \frac{\partial \varphi}{\partial t} - \alpha \Delta^2 \varphi + \boldsymbol{m}^* \cdot \nabla \varphi + a\varphi,$$

and the desired state is

$$\varphi_d = \varphi - \frac{1}{\gamma}\left(-\frac{\partial \phi}{\partial t} - \alpha\Delta^2\phi - \boldsymbol{m}^* \cdot \nabla\phi + a\phi\right).$$

With this construction, $\boldsymbol{m}^*$ is the exact optimal control.

In numerical simulations, the coefficient associated with the biharmonic diffusion operator is fixed to $\alpha = 10^{-3}$, while the reaction parameter is taken as $a = 1$, the initial control is $(0, 0)$, and the regularization and tracking parameters appearing in the cost functional are initially selected as $\gamma_0 = 100$.

Remark 7.1. *The small-data assumption is essential in the present analysis, since it allows us to control the nonlinear terms and derive the stability and uniqueness estimates required for the optimal control problem. Moreover, this assumption is consistent with the physical nature of the model, which is intended to describe a regime of moderate amplitudes and bounded perturbations. Extending the results to arbitrary-size data would correspond to a more strongly nonlinear regime and remains beyond the scope of this work.*

The spatial temporal domain $\Theta \times (0, T) = (0, 1)^2 \times (0, 1)$ is discretized using a uniform grid with

$$N_x = 1000, \quad N_y = 100, \quad \text{and } N_t = 1000.$$

This discretization ensures an accurate approximation of the analytical solutions used in the numerical experiments.

Furthermore, the regularization parameter is chosen as a decreasing sequence

$$\varepsilon_n = \frac{1}{n}, \qquad n \geq 1,$$

which allows the penalized formulation to approximate the minimum energy control problem as $n \to \infty$.

Figure 1 presents the initial distributions of the state φ and the desired state φ_d at $t = 0$. One can clearly observe a noticeable discrepancy between the two profiles before the convergence of the algorithm. This observation is confirmed by the absolute and relative errors computed, which are equal to 8.375466×10^{-2} and 1.475175×10^{-1}, respectively. Hence, the figure highlights the initial mismatch between the state of the system and the target configuration, providing a reference point to assess the efficiency of the proposed optimal control procedure.

To evaluate the accuracy of the numerical approximation independently of the magnitude of the solution, we consider the tracking error $E(t) = \left(\int_\Theta |\varphi(x,t) - \varphi_d(x,t)|^2\, dx\right)^{\frac{1}{2}}$, and the relative tracking error defined by $E_{\text{rel}}(t) = \dfrac{\|\varphi(\cdot,t) - \varphi_d(\cdot,t)\|_{L^2(\Theta)}}{\|\varphi_d(\cdot,t)\|_{L^2(\Theta)}} \leq 10^{-04}$.

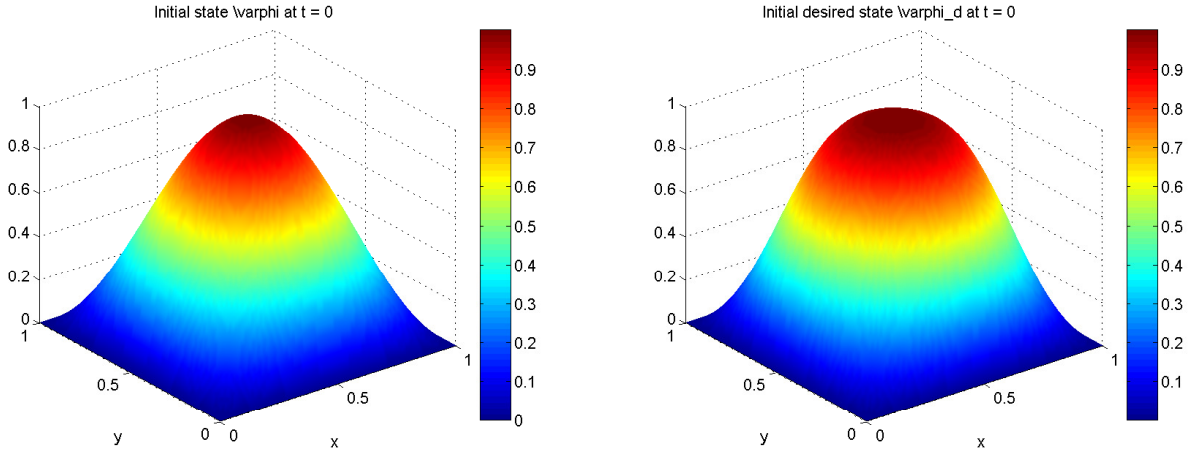

Figure 1. Initial profiles of the state φ and the desired state φ_d at $t = 0$, illustrating the discrepancy between the uncontrolled initial configuration and the prescribed target. The corresponding absolute and relative errors are 8.375466×10^{-2} and 1.475175×10^{-1}, respectively, which confirm that the system is initially far from the desired state before the convergence of the proposed control procedure.

7.2. Simulation results

In the following, we present the findings of the numerical simulation illustrating the performance and convergence properties of the proposed optimal control approach. The proposed conjugate gradient algorithm 6.2 is applied to solve the optimal control problem 2.2. The error curve Figure 8 demonstrates a progressive decrease during simulation, indicating that the computed state approaches the desired configuration. The convergence regime starts around iteration $k = 972$, corresponding to time $t = 0.97197$.

Figure 2 displays the desired computed state φ_d at three representative times chosen during the iterative process. These times are selected to illustrate the progressive evolution of the surface rather than to indicate any special physical threshold. One can observe a gradual improvement in the shape of the profile as the process advances, showing how the surface evolves toward the final converged configuration. This figure therefore provides a visual illustration of the progression of the algorithm toward the convergence state.

Figure 3 presents the computed state φ at three representative times chosen during the iterative process. These snapshots show the gradual evolution of the state surface as the algorithm progresses, illustrating its progressive adjustment toward the final converged configuration.

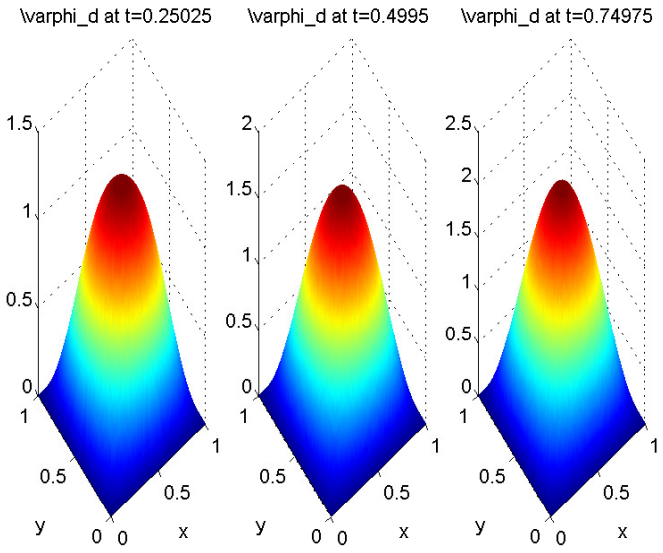

Figure 2. Computed desired state φ_d at three representative times $t = 0.25$, $t = 0.49$, and $t = 0.74$, illustrating the evolution of the target profile during the iterative process.

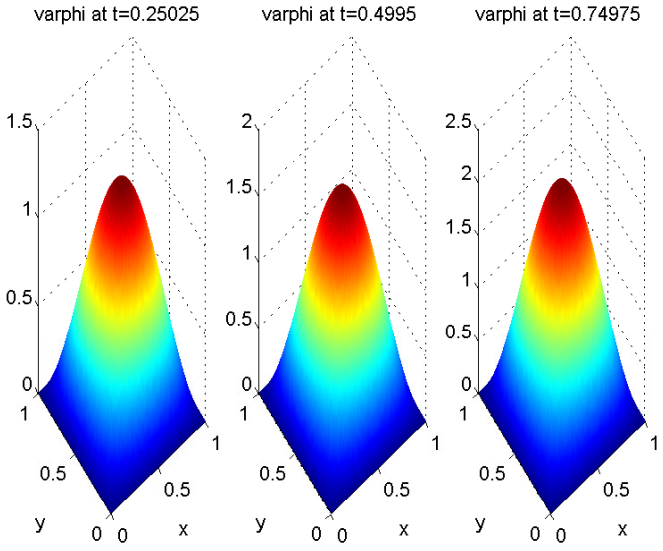

Figure 3. Computed state φ at three representative times $t = 0.25$, $t = 0.49$, and $t = 0.74$. The figure illustrates the progressive evolution of the state surface during the iterative process.

Figure 4 presents the adjoint state computed ϕ at three representative times chosen during the iterative process. As the adjoint state is directly involved in the characterization of the optimal control, its behavior is of particular interest. One can observe a progressive decrease in its amplitude, which reflects the stabilization of the optimality system and supports the convergence of the control toward its limiting minimum-energy configuration.

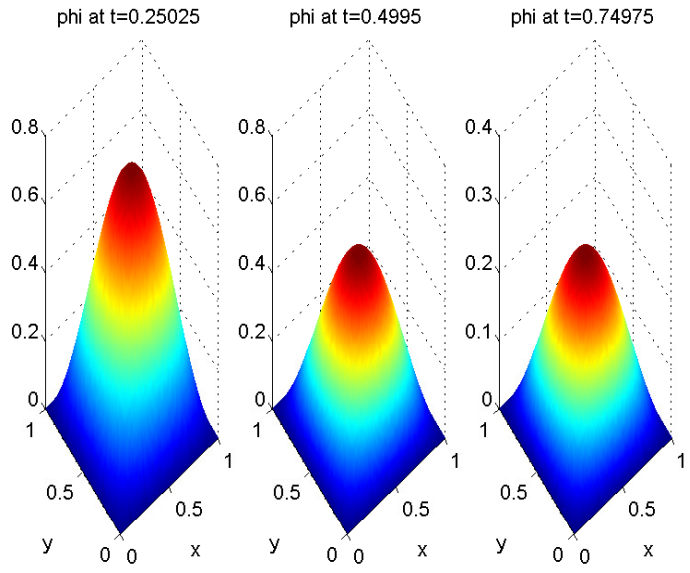

Figure 4. Computed adjoint state ϕ at three representative times $t = 0.25$, $t = 0.49$, and $t = 0.74$. The figure illustrates the evolution of the adjoint variable during the iterative process and shows the progressive reduction of its amplitude as the algorithm approaches convergence.

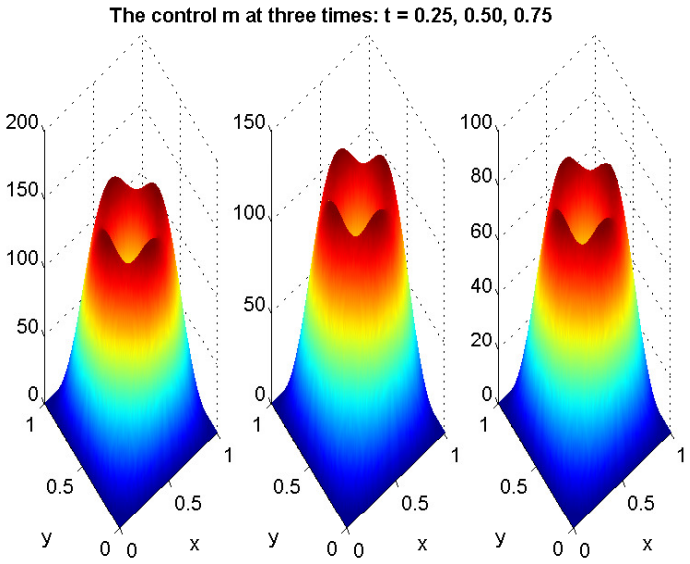

Figure 5. Computed control m at three representative times $t = 0.25$, $t = 0.49$, and $t = 0.74$. The figure illustrates the evolution of the control profile during the iterative process and shows the progressive reduction of its amplitude as the algorithm approaches the minimum-energy configuration.

Figure 5 shows the optimal control m at $t = 0.25$, $t = 0.49$, and $t = 0.74$. The evolution of the control illustrates how the algorithm gradually adjusts the actuation to drive the state toward the desired configuration while maintaining a stable energy distribution.

Figure 5 shows the calculated control m at three representative times, namely, $t = 0.25$, $t = 0.49$, and $t = 0.74$. These snapshots illustrate the evolution of the control surface during the iterative process. The progressive decrease in amplitude reveals the reduction in associated energy and supports the convergence of the algorithm toward a limiting optimal control of minimum energy.

Figure 6 shows the evolution in time of the tracking error $E(t)$. Its monotone decrease indicates that the computed state φ is progressively driven toward the desired state φ_d. The numerical results reveal that the proposed algorithm achieves a minimum tracking error

$$E_{\min} = 10^{-4},$$

and that the maximum relative error satisfies

$$E_{\text{rel}}^{\max} = 7.66 \times 10^{-5}.$$

This behavior provides clear numerical evidence of the precision, stability, and convergence of the proposed optimal control method.

Figure 6 presents the evolution of the tracking error $E(t)$ during the iterative process. One can observe a progressive decay of the error over time, which indicates that the computed state φ is increasingly close to the desired state φ_d. This decreasing behavior provides clear numerical evidence for the convergence and effectiveness of the proposed optimal control algorithm.

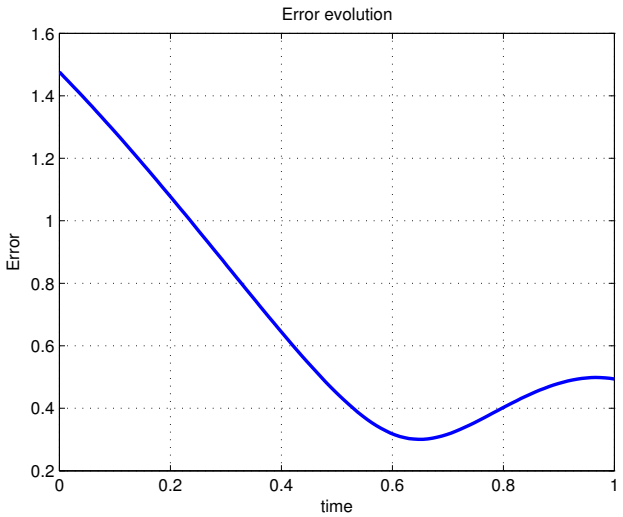

Figure 6. Evolution of the tracking error $E(t)$ during the iterative process, illustrating its progressive decay over time and confirming the convergence of the proposed optimal control algorithm.

To investigate the influence of the tracking parameter γ on the performance of the proposed optimal control algorithm, several numerical experiments were carried out. The results obtained are summarized in Table 1.

Table 1. Influence of the tracking parameter γ on the numerical accuracy of the proposed method.

γ	**Minimum error** $E_{\min}$	**Relative error** E_{rel}
1.0×10^2	2.51×10^{-3}	1.32×10^{-3}
2.51×10^3	1.00×10^{-4}	7.66×10^{-5}

The results clearly show that increasing the parameter γ significantly improves the accuracy of the tracking. In particular, the minimum error decreases from the order 10^{-3} to 10^{-4}, while the relative error reaches 7.66×10^{-5}, which confirms the stability and efficiency of the proposed numerical approach. The convergence behavior of the proposed algorithm can be clearly observed from the evolution of the tracking error. In particular, the convergence regime starts with iteration $k = 972$, corresponding to time $t = 0.97197$, where the error reaches the prescribed tolerance level $E(t) \leq 10^{-4}$. From this point on, the numerical solution remains stable and the state variable φ stays very close to the desired state φ_d, confirming the effectiveness and stability of the proposed optimal control strategy. To further illustrate the stability of the proposed algorithm, Table 2 reports the numerical values obtained during the last iterations of the simulation.

Table 2. Numerical values obtained during the last iterations of the algorithm.

Iteration k	**Time** t	**Error**	**Mean** (φ)	**Mean** (φ_d)
996	0.99600	1.94×10^{-4}	1.069733	1.069579
997	0.99700	1.95×10^{-4}	1.070805	1.070649
998	0.99800	1.96×10^{-4}	1.071877	1.071720
999	0.99900	1.97×10^{-4}	1.072951	1.072793
1000	1.00000	1.97×10^{-4}	1.074025	1.073868

The results show that the values of the state φ and the desired state φ_d become nearly identical as the iteration progresses. This behavior confirms that the algorithm has reached a stable convergence regime and that the optimal control successfully drives the system toward the desired configuration.

Figure 7 compares the computed state φ with the desired state φ_d after the convergence of the algorithm. One can observe that the two surfaces almost overlap at iteration $k = 972$, corresponding to $t = 0.97197$. This close agreement indicates that the proposed control successfully steers the system toward the prescribed target and confirms the accuracy of the numerical procedure.

Figure 8 displays the evolution of absolute and relative tracking errors during the iterative process. One can observe that both curves decrease progressively over time, which indicates that the discrepancy between the computed state and the desired state is steadily reduced. This behavior provides numerical evidence of the convergence and stability of the proposed algorithm.

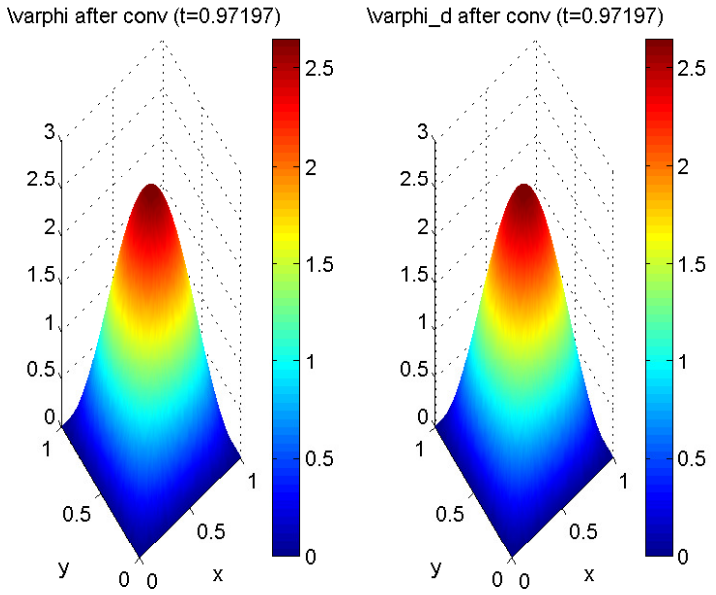

Figure 7. Comparison between the computed state φ and the desired state φ_d after convergence of the algorithm, at iteration $k = 972$ corresponding to $t = 0.97197$. The two surfaces almost overlap, confirming that the proposed control procedure effectively drives the system toward the prescribed target state.

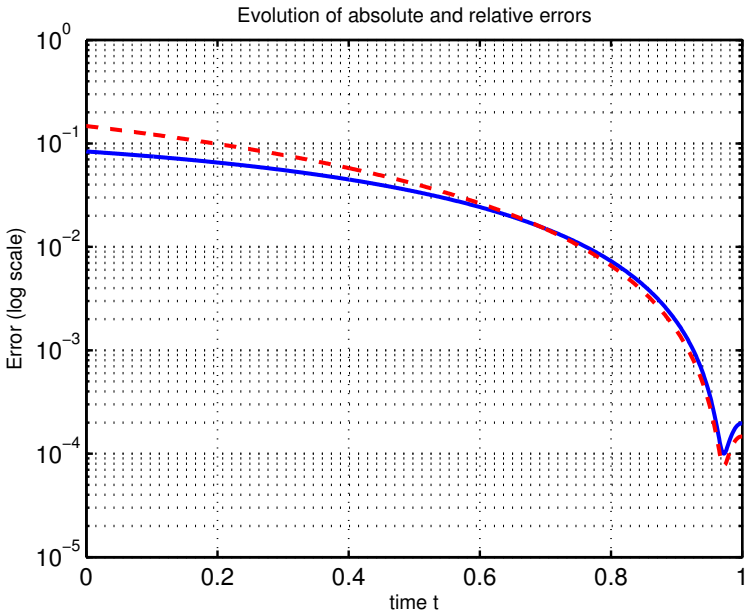

Figure 8. Evolution of the absolute (blue solid line) and relative (red dashed line) tracking errors during the iterative process. The progressive decrease of both quantities confirms the convergence and stability of the proposed algorithm.

7.3. *Numerical illustration and interpretation of the converged control*

The numerical simulations are presented in order to illustrate the behavior of the control generated by the proposed iterative procedure. The objective is not only to verify the convergence of the algorithm, but also to analyze the evolution of the control once convergence is achieved.

The control appearing in the model considered depends on a regularization parameter ε. This parameter directly influences the amplitude of the control action: Small values of ε produce stronger controls, while larger values lead to smoother and weaker control fields.

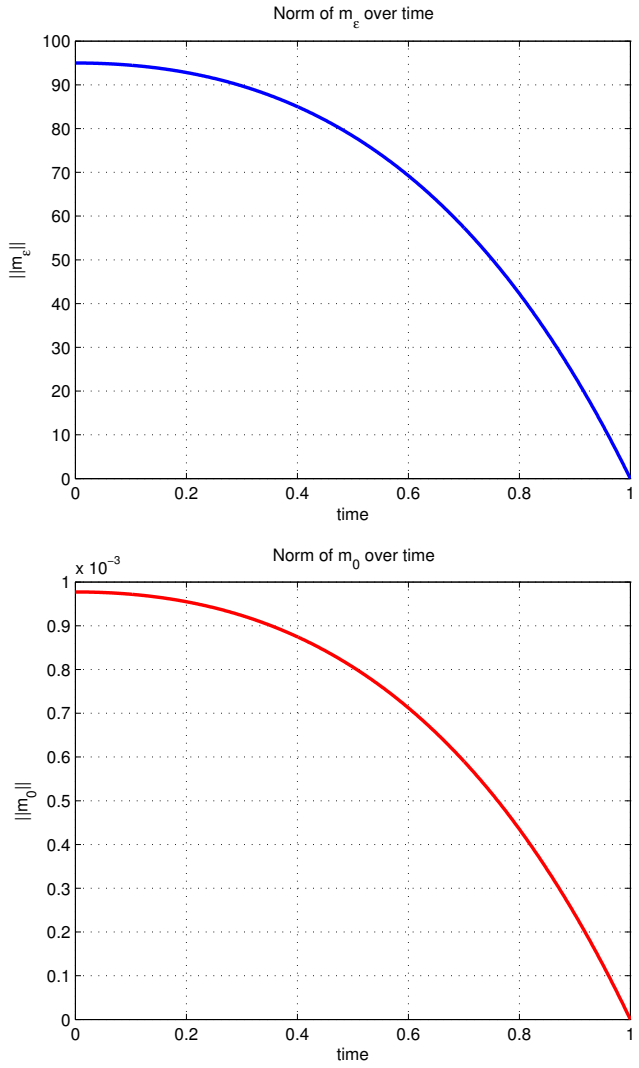

Figure 9. Evolution of the absolute (blue line) and relative (red line) tracking errors during the iterative process. The progressive decrease of both quantities confirms the convergence and stability of the proposed algorithm. In addition, the comparison between the control m_ϵ and its limit m_0 shows a significant reduction in amplitude, with m_ϵ decreasing from about 95 to 10, while m_0 varies from 10^{-3} to 10^{-4}. This behavior indicates that the limiting control realizes a minimum-energy configuration.

Figure 9 shows the evolution of absolute and relative tracking errors during the iterative process. Both curves decrease steadily, which confirms the convergence and numerical stability of the proposed method. Moreover, the behavior of the control further supports this conclusion: the approximate control m_ϵ exhibits amplitudes ranging from about 95 to 10, while its limit control m_0 remains much smaller, between 10^{-3} and 10^{-4}. This clear reduction shows that the limiting control is energetically more efficient and confirms that the algorithm converges toward a minimum-energy control.

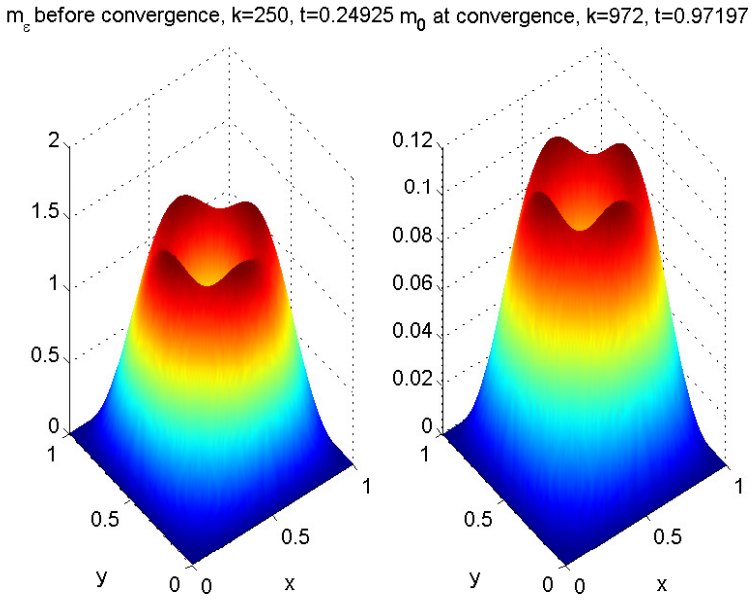

Figure 10. Spatial comparison between the control m_ϵ before convergence and the limiting control m_0 at convergence. The snapshots are taken at iteration $k = 250$ ($t = 0.24925$) for m_ϵ and at iteration $k = 972$ ($t = 0.97197$) for m_0.

Figure 10 presents a spatial comparison between the control m_ϵ before convergence and its limit control m_0 at convergence. More precisely, the control m_ϵ is displayed at iteration $k = 250$, corresponding to $t = 0.24925$, while the limiting control m_0 is shown at the convergence step $k = 972$, corresponding to $t = 0.97197$. The two meshes clearly reveal a significant reduction in the amplitude and magnitude of the control at convergence. This behavior indicates that the algorithm progressively decreases the control effort and supports the minimum-energy character of the limiting control. The convergence iteration k_{conv} is defined as the first time step for which the error becomes sufficiently small. At this stage, the controlled system accurately follows the desired trajectory. After convergence is detected, a modified parameter is introduced using the convergence iteration number,

$$\varepsilon_0 = k_{\text{conv}}.$$

This choice increases the regularization level of the control and produces a new control field with reduced amplitude. Consequently, although the tracking objective remains satisfied, the control effort becomes significantly smaller.

To further analyze this behavior, the temporal evolution of the control norms is used.

$$\|m_\varepsilon(t)\| \quad \text{and} \quad \|m_0(t)\|$$

are computed over the time interval $[0, T]$. This behavior admits an important interpretation. Once the desired trajectory has been reached, the algorithm implicitly approaches a configuration requiring minimal control effort. Therefore, the post-convergence control m_0 can be interpreted as an approximation of a minimum-energy control associated with the system.

Moreover, this numerical stabilization is consistent with the theoretical uniqueness properties established for the optimal control problem. When the algorithm approaches the optimal regime, successive iterations produce only negligible variations, indicating convergence toward a unique admissible control.

In general, the numerical experiments demonstrate that the proposed approach simultaneously ensures accurate trajectory tracking and reduction of control energy after convergence, confirming the effectiveness and stability of the proposed control strategy.

7.4. Discussion

The present study investigates an optimal control problem governed by a fourth-order advection–reaction–diffusion system in which the control variable acts through a drift mechanism. Such models naturally arise in several applications where transport processes can be influenced through the modification of a velocity or convection field.

The main objective of the proposed framework is to steer the state of the system toward a prescribed desired configuration while minimizing the associated control energy. In contrast to classical additive control problems, the model considered leads to a bilinear coupling between the control and the state equation. This interaction increases the mathematical complexity of the optimization problem, since the control simultaneously affects both transport and diffusion phenomena.

Consequently, the construction of stable and efficient numerical methods becomes an essential aspect of the analysis. To address this difficulty, an optimality system composed of state and adjoint equations has been derived and numerically solved using a conjugate gradient algorithm. An important advantage of this approach is that each iteration requires solving only one state equation and one adjoint equation, which significantly reduces the computational cost while preserving the stability of the iterative procedure.

The numerical simulations clearly demonstrate the effectiveness of the proposed method. In the initial stage, there is a noticeable discrepancy between the state φ and the desired state φ_d. As the iterations progress, the optimal control gradually reduces this mismatch, leading to a continuous decay of the tracking error. The evolution of the error curve confirms the convergence of the algorithm, with the convergence regime appearing around the iteration $k = 972$, corresponding to the time $t = 0.97197$. Furthermore, the comparison between the initial configuration and the post-convergence results shows that the computed state nearly coincides with the desired configuration. The relative error obtained of order 10^{-5} highlights the high precision and robustness of the proposed numerical approach.

The smooth spatial evolution observed for both the adjoint variable and the optimal control also confirms the numerical stability of the method.

The numerical experiments reveal that after the convergence of the proposed iterative procedure, the control magnitude significantly decreases while preserving the tracking accuracy. This behavior suggests that the algorithm progressively eliminates unnecessary control effort once the desired trajectory is reached. In this sense, the post-convergence control can be interpreted as an approximation of a stabilized or minimum-energy control configuration. Such an observation is consistent with the

theoretical properties of the optimal control problem, where convergence toward a unique admissible control naturally leads to reduced control energy and improved stability of the controlled dynamics.

In general, the results obtained validate the theoretical formulation and demonstrate that the proposed optimal control strategy provides an efficient and reliable framework for solving bilinear control problems governed by higher-order diffusion models.

The developed approach can be extended to several practical applications, including pollutant transport, thermal convection, and population dispersal dynamics.

8. Conclusions

In this work, we studied a minimum-energy optimal control problem governed by a fourth-order advection–reaction–diffusion equation in which the control acts through a drift field in the advection term. This bilinear control structure makes the problem more delicate than in the classical additive-control case, since it directly affects the transport mechanism of the system and creates additional analytical and numerical difficulties.

The main contribution of the paper is the characterization of the minimum-energy control as the limit of a family of penalized optimal control problems. This approach provides a constructive and stable framework for approximating the optimal solution and gives a natural interpretation of the minimum energy control for higher-order transport models.

Another important theoretical result is the uniqueness of the optimal control under a suitable additional condition. Since uniqueness is not generally guaranteed in bilinear control problems, this result is significant both analytically and numerically. It reinforces the well-posedness of the problem and supports the convergence of the proposed optimization procedure.

From a numerical point of view, the associated optimality system was solved by means of a conjugate gradient algorithm that required, at each iteration, only the solution of the state equation and the adjoint equation. The numerical simulations confirmed the effectiveness of the method in driving the system toward the desired state while reducing the control energy. In particular, the decay of the tracking error, the small relative error observed after convergence, and the comparison between m_ϵ and its limit control m_0 illustrate the stability, precision, and minimum-energy character of the proposed approach.

Overall, the present work provides a new contribution to the analysis and computation of minimum-energy controls for fourth-order advection–reaction–diffusion systems. Beyond its theoretical interest, the proposed framework may be relevant for applications involving transport-dominated processes such as pollutant propagation, thermal convection, and population dynamics. Possible directions for future research include the treatment of more general nonlinear models, the extension to larger data, the development of adaptive numerical discretizations, and the application of the method to more realistic geometries and boundary conditions.

Author contributions

All authors contributed equally to this work. All authors have read and agreed to the published version of the manuscript.

Use of Generative-AI tools declaration

The authors declare they have not used Artificial Intelligence (AI) tools in the creation of this article.

Acknowledgments

This work was funded by the Deanship of Graduate Studies and Scientific Research at Jouf University under grant no. (DGSSR-2025-NF-02-011).

Conflicts of interest

The authors declare that they have no conflict of interest.

References

1. J. L. Lions, *Optimal control of systems governed by partial differential equations*, Berlin: Springer, **170** (1971).
2. A. Moussa, Some variants of the classical Aubin–Lions lemma, *J. Evol. Equ.*, **16** (2016), 65–93. https://doi.org/10.1007/s00028-015-0293-3
3. J. L. Lions, E. Magenes, *Problèmes aux limites non-homogènes et applications*, Paris: Dunod, **1** (1968).
4. J. L. Lions, E. Magenes, *Non-homogeneous boundary value problems and applications*, Berlin: Springer, **1** (2012).
5. F. Tröltzsch, *Optimal control of partial differential equations: Theory, methods and applications*, Providence: American Mathematical Society, **112** (2010).
6. R. Glowinski, J. L. Lions, J. He, *Exact and approximate controllability for distributed parameter systems: A numerical approach*, Cambridge: Cambridge University Press, 2010.
7. H. Brezis, *Functional analysis, Sobolev spaces and partial differential equations*, New York: Springer, **2** (2011).
8. E. Zuazua, Controllability and observability of partial differential equations: Some results and open problems, *Handbook Differ. Eq. Evol. Eq.*, **3** (2007), 527–621. https://doi.org/10.1016/S1874-5717(07)80010-7
9. A. Y. Khapalov, *Controllability of partial differential equations governed by multiplicative controls*, Heidelberg: Springer, 2010.
10. P. Cannarsa, G. Floridia, A. Y. Khapalov, Multiplicative controllability for semilinear reaction–diffusion equations with finitely many changes of sign, *J. Math. Pure. Appl.*, **108** (2017), 425–458. https://doi.org/10.1016/j.matpur.2017.07.002
11. K. Ito, K. Kunisch, Optimal bilinear control of an abstract Schrödinger equation, *SIAM J. Control Optim.*, **46** (2007), 274–287. https://doi.org/10.1137/05064254X

12. E. Zerrik, M. O. Sidi, Regional controllability for infinite-dimensional bilinear systems: Approach and simulations, *Int. J. Control*, **84** (2011), 2108–2116. https://doi.org/10.1080/00207179.2011.632442
13. K. Ztot, E. Zerrik, H. Bourray, Regional control problem for distributed bilinear systems, *Int. J. Ap. Mat. Com.-Pol.*, **21** (2011), 499–508.
14. S. Lenhart, J. T. Workman, *Optimal control applied to biological models*, Boca Raton: Chapman & Hall/CRC, 2007.
15. R. Glowinski, Y. Song, X. Yuan, H. Yue, Bilinear optimal control of an advection-reaction-diffusion system, *SIAM Rev.*, **64** (2022), 392–421. https://doi.org/10.1137/21M1389778
16. A. V. Fursikov, *Optimal control of distributed systems. Theory and applications*, Translations of Mathematical Monographs, American Mathematical Society, 1999.
17. R. Becker, B. Vexler, Optimal control of the convection–diffusion equation using stabilized finite element methods, *Numer. Math.*, **106** (2007), 349–367.
18. A. Kröner, B. Vexler, A priori error estimates for elliptic optimal control problems with a bilinear state equation, *J. Comput. Appl. Math.*, **230** (2009), 781–802. https://doi.org/10.1016/j.cam.2009.01.023
19. A. Borzì, E. J. Park, M. Vallejos Lass, Multigrid optimization methods for the optimal control of convection–diffusion problems with bilinear control, *J. Optimiz. Theory App.*, **168** (2016), 510–533. https://doi.org/10.1007/s10957-015-0791-z
20. A. Fleig, R. Guglielmi, Optimal control of the Fokker–Planck equation with space-dependent controls, *J. Optimiz. Theory App.*, **174** (2017), 408–427. https://doi.org/10.1007/s10957-017-1120-5
21. R. Glowinski, *Variational methods for the numerical solution of nonlinear elliptic problems*, Philadelphia: Society for Industrial and Applied Mathematics (SIAM), 2015.
22. F. Bersetche, F. Fuica, E. Otárola, D. Quero, Bilinear optimal control for the fractional Laplacian: Analysis and discretization, *SIAM J. Numer. Anal.*, **62** (2024), 1344–1371. https://doi.org/10.1137/23M154947X
23. C. Kenne, L. Djomegne, J. Larrouy, Bilinear optimal control of a one-dimensional degenerate parabolic equation with a nonlocal term, *Math. Method. Appl. Sci.*, **47** (2024), 11670–11692. https://doi.org/10.1002/mma.10148
24. F. Achab, A. Hafdallah, A. Ayadi, I. Rezzoug, Optimal control of a bilinear distributed system with incomplete data, *Bound Value Probl.*, **2025** (2025), 159. https://doi.org/10.1186/s13661-025-02113-8
25. N. E. Boukhari, E. H. Zerrik, Optimal control of a class of bilinear systems with unbounded control operators: A semigroup approach, *J. Control Decis.*, **2025** (2025), 1–13. https://doi.org/10.1080/23307706.2025.2566994
26. G. Mophou, Bilinear optimal control for a nonlinear parabolic equation with nonlocal time dependence, *Axioms*, **14** (2025), 38. https://doi.org/10.3390/axioms14010038
27. G. Mophou, C. Kenne, M. Warma, Bilinear optimal control for a fractional diffusive equation, *Optimization*, **75** (2026), 267–293. https://doi.org/10.1080/02331934.2024.2421384

28. E. Otárola, D. Quero, M. Sasso, A bilinear pointwise tracking optimal control problem for semilinear PDEs, *J. Comput. Phys.*, **2026** (2026). https://doi.org/10.2139/ssrn.5499625

29. A. Albarrak, M. Benoudi, M. O. Sidi, I. O. Ahmed, H. O. Sidi, An inverse problem for recovering a time-dependent source in time fractional diffusion–wave models governed by the integral fractional Laplacian, *Chaos Soliton. Fract.*, **205** (2026), 117887. https://doi.org/10.1016/j.chaos.2026.117887

30. E. S. Baranovskii, R. V. Brizitskii, Z. Y. Saritskaia, Optimal control problems for the reaction–diffusion–convection equation with variable coefficients, *Nonlinear Anal.-Real*, **75** (2024), 103979. https://doi.org/10.1016/j.nonrwa.2023.103979

31. M. Johnson, M. M. Raja, V. Vijayakumar, A. Shukla, Optimal control results for fractional differential hemivariational inequalities of order $r \in (1, 2)$, *Optimization*, **74** (2025), 1425–1449. https://doi.org/10.1080/02331934.2024.2306304

32. M. M. Raja, V. Vijayakumar, C.-W. Tsai, K. C. Veluvolu, Optimal control strategies and continuous dependence for stochastic Hilfer fractional systems with delay: A Volterra–Fredholm integro-differential approach, *Optim. Contr. Appl. Met.*, **46** (2025), 2708–2726. https://doi.org/10.1002/oca.70024

33. M. M. Raja, V. Vijayakumar, A. Shukla, K. S. Nisar, N. Sakthivel, K. Kaliraj, Optimal control and approximate controllability for fractional integrodifferential evolution equations with infinite delay of order $r \in (1, 2)$, *Optim. Contr. Appl. Met.*, **43** (2022), 996–1019. https://doi.org/10.1002/oca.2867

34. N. I. Chaudhary, M. A. Z. Raja, Z. A. Khan, A. Mehmood, S. M. Shah, Design of fractional hierarchical gradient descent algorithm for parameter estimation of nonlinear control autoregressive systems, *Chaos Soliton. Fract.*, **157** (2022), 111913. https://doi.org/10.1016/j.chaos.2022.111913

35. N. I. Chaudhary, Z. A. Khan, A. K. Kiani, M. A. Z. Raja, I. I. Chaudhary, C. M. Pinto, Design of auxiliary model based normalized fractional gradient algorithm for nonlinear output-error systems, *Chaos Soliton. Fract.*, **163** (2022), 112611. https://doi.org/10.1016/j.chaos.2022.112611

AIMS Press